



中国科学院上海天文台



中国科学院大学
University of Chinese Academy of Sciences

空间飞行器精密定轨

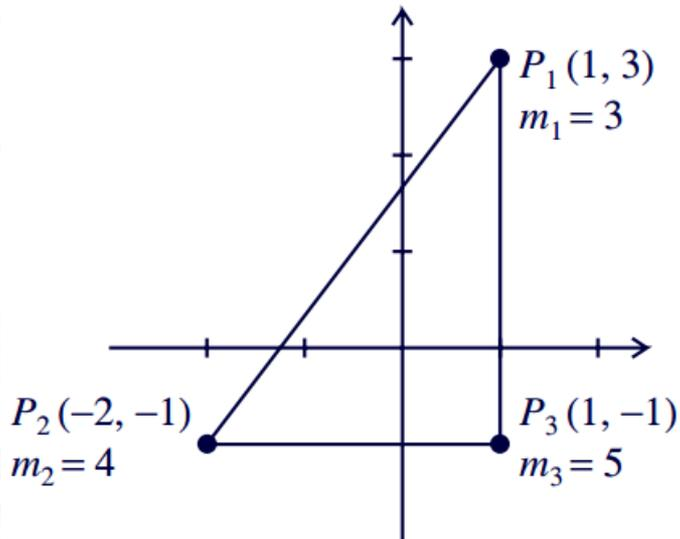
宋叶志

2021秋季 作业邮箱: song.yz@foxmail.com
课件地址: <http://202.127.29.4/astrodynamics>

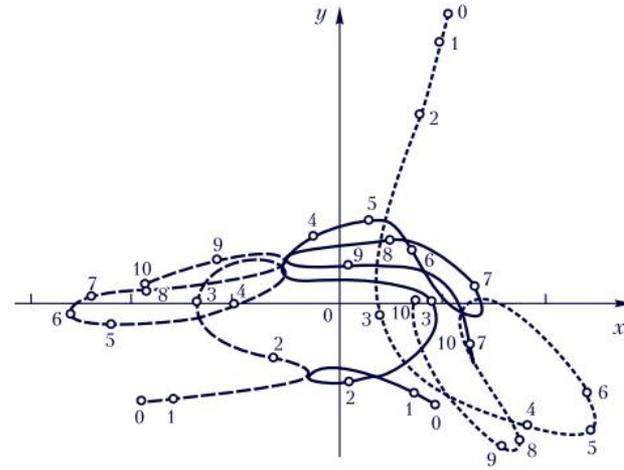
第七讲 三体问题及应用

- 一. 一般三体问题
- 二. 圆形限制性三体问题
- 三. 平动点及稳定性
- 四. 周期轨道不变流形
- 五. Halo轨道
- 六. Hill限制性三体问题及周期解
- 七. DRO轨道动力学

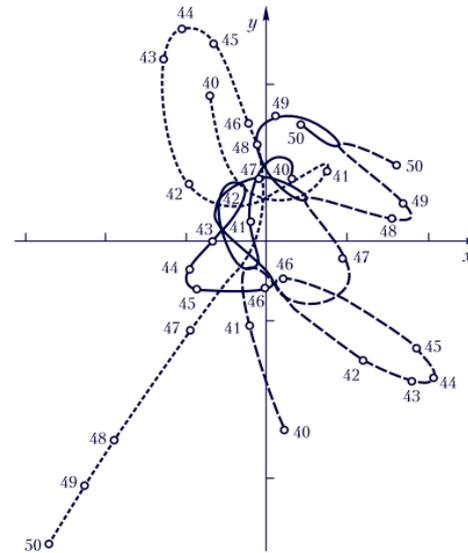
Pythagorean three-body problem



Initial configuration of the Pythagorean problem.

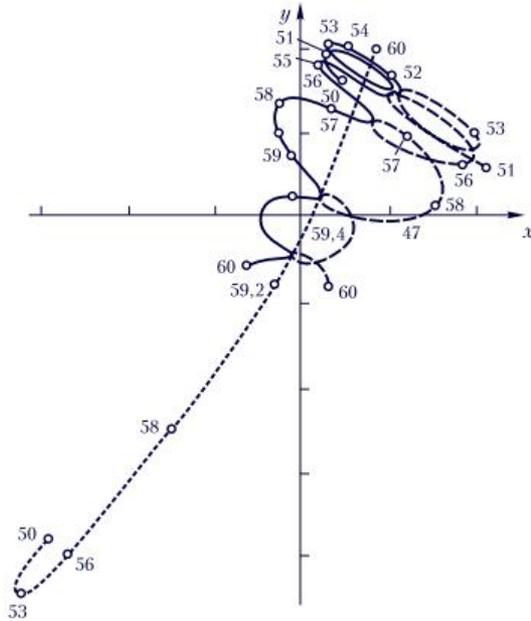


Motion of gravitating masses in the Pythagorean three-body problem in

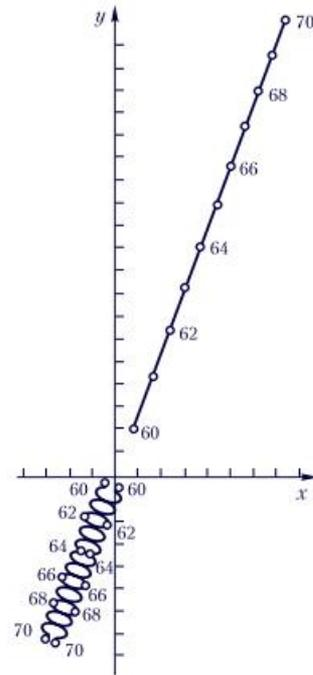


Form of the orbits in the Pythagorean three-body problem in the time interval from $t = 40$ to $t = 50$

Pythagorean three-body problem



Evolution of the orbits of the Pythagorean three-body problem in the time interval from $t = 50$ to $t = 60$



Formation of a double star in the Pythagorean three-body problem (from $t = 60$ to $t = 70$)

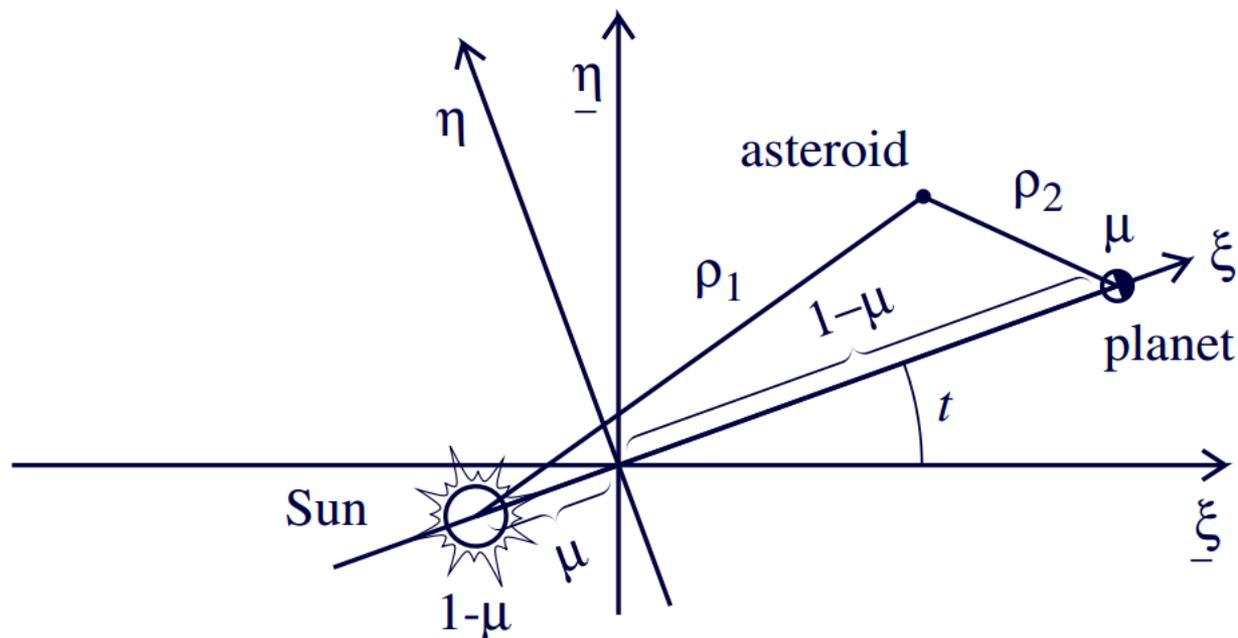


圆形限制性三体问题

$$L = \frac{1}{2}(\dot{X}^2 + \dot{Y}^2 + \dot{Z}^2) - U(X, Y, Z, t) \quad U(x, y, z) = -\frac{\mu_1}{r_1} - \frac{\mu_2}{r_2} - \frac{1}{2}\mu_1\mu_2$$

$$\frac{1}{2}(\dot{X}^2 + \dot{Y}^2 + \dot{Z}^2) = \frac{1}{2}[(\dot{x} - y)^2 + (\dot{y} + x)^2 + \dot{z}^2]$$

$$\frac{d}{dt} \frac{\partial L}{\partial \dot{\mathbf{q}}} - \frac{\partial L}{\partial \mathbf{q}} = \mathbf{0}$$



小天体运动方程

$$\begin{cases} \ddot{x} - 2\dot{y} = -\frac{\partial \bar{U}}{\partial x} \\ \ddot{y} + 2\dot{x} = -\frac{\partial \bar{U}}{\partial y} \\ \ddot{z} = -\frac{\partial \bar{U}}{\partial z} \end{cases}$$

$$\begin{cases} \bar{U} = -\frac{1}{2}(x^2 + y^2) - \frac{\mu_1}{r_1} - \frac{\mu_2}{r_2} - \frac{1}{2}\mu_1\mu_2 \\ = -\frac{1}{2}(\mu_1 x^2 + \mu_2 y^2) - \frac{\mu_1}{r_1} - \frac{\mu_2}{r_2} \\ r_1 = [(x + \mu_2)^2 + y^2 + z^2]^{\frac{1}{2}} \\ r_2 = [(x - \mu_1)^2 + y^2 + z^2]^{\frac{1}{2}} \end{cases}$$

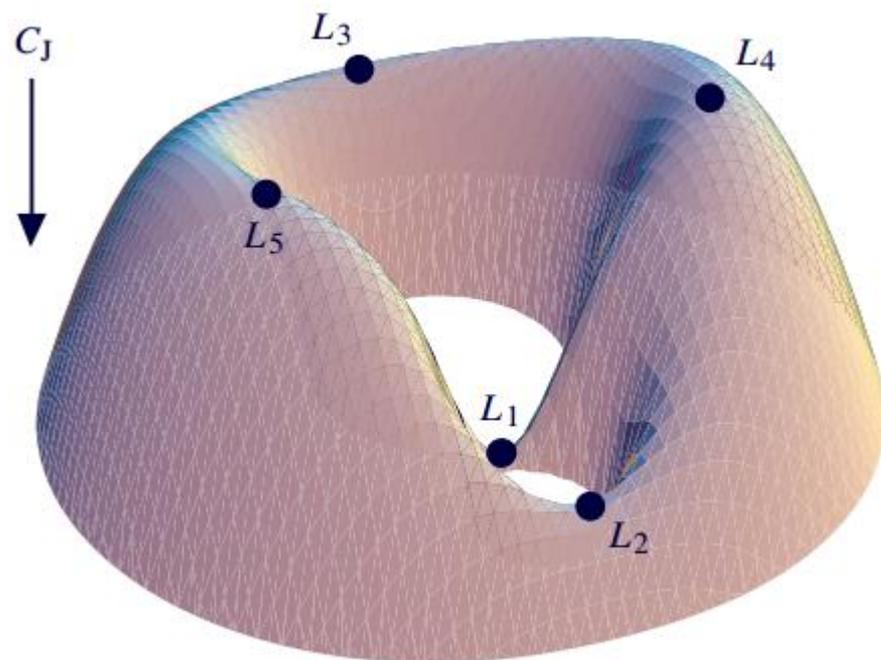
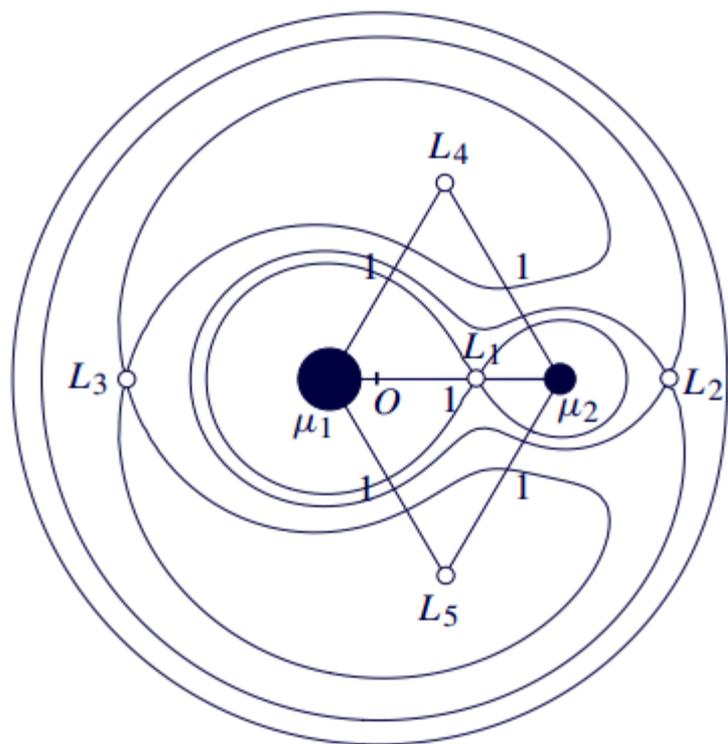
$$\begin{cases} [M] = M_1 + M_2, \\ [L] = a_{12}, \\ [T] = [a_{12}^3 / G(M_1 + M_2)]^{1/2} = 1/n. \end{cases}$$

$$G = 1$$

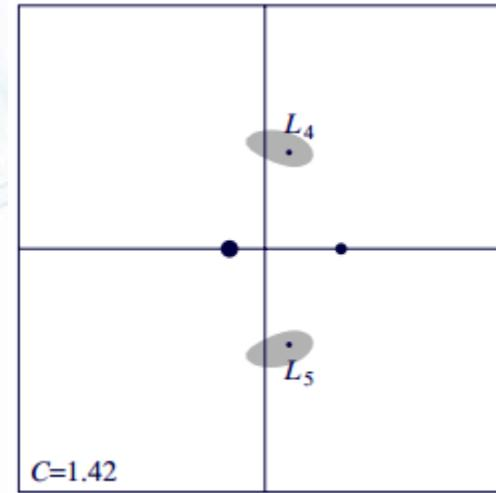
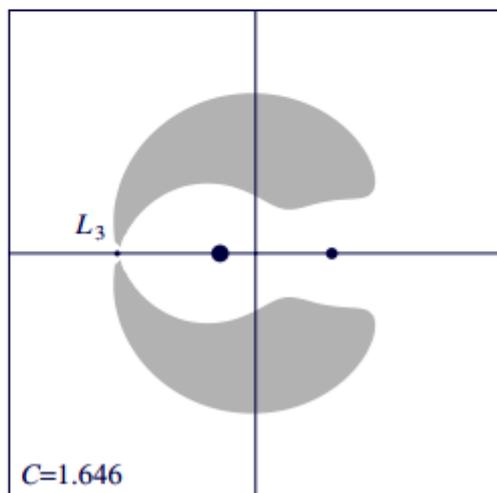
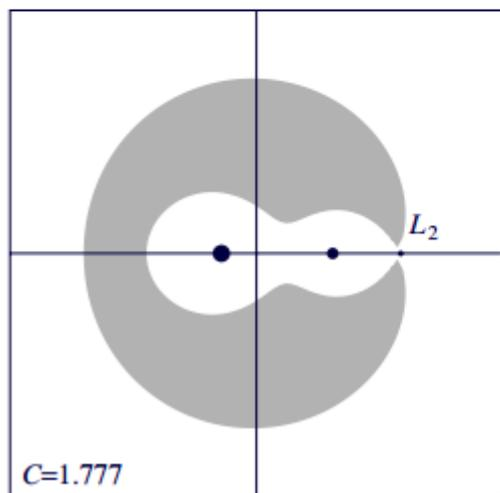
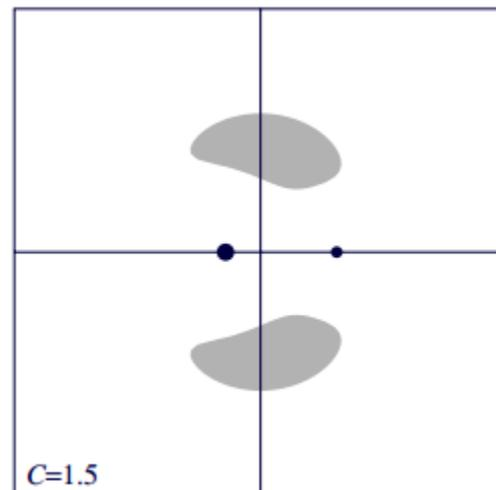
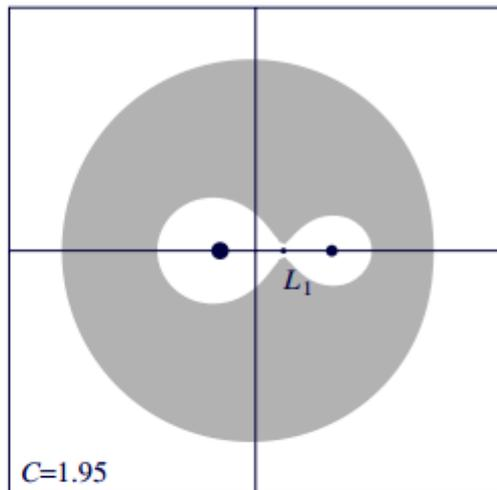
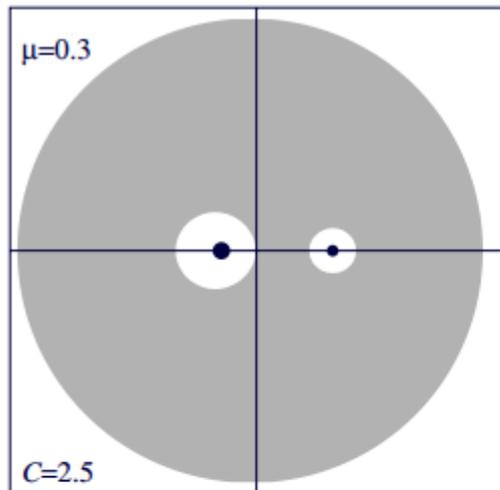
雅可比积分常数与能量曲面

$$\dot{x}\ddot{x} + \dot{y}\ddot{y} + \dot{z}\ddot{z} = \frac{\partial U}{\partial x}\dot{x} + \frac{\partial U}{\partial y}\dot{y} + \frac{\partial U}{\partial z}\dot{z} = \frac{dU}{dt}$$

$$C_J = n^2(x^2 + y^2) + 2\left(\frac{\mu_1}{r_1} + \frac{\mu_2}{r_2}\right) - \dot{x}^2 - \dot{y}^2 - \dot{z}^2.$$



飞行禁区



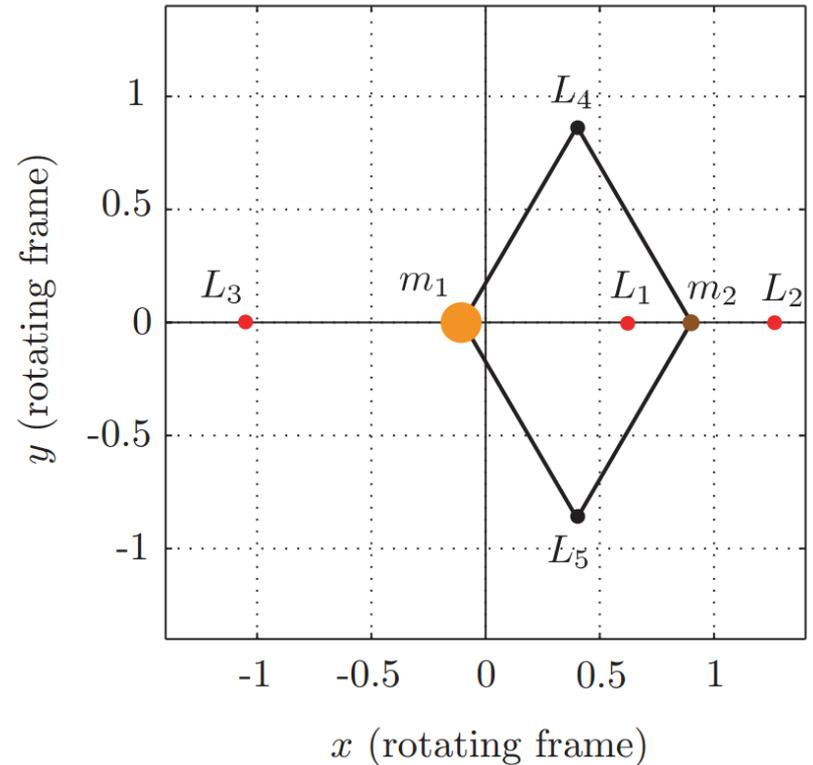
平动点位置

$$\begin{cases} \Omega_x = x - \frac{(1-\mu)(x-\mu)}{r_1^3} - \frac{\mu(x+1-\mu)}{r_2^3} = 0 \\ \Omega_y = y \left(1 - \frac{1-\mu}{r_1^3} - \frac{\mu}{r_2^3} \right) = 0, \\ \Omega_z = -z \left(\frac{1-\mu}{r_1^3} + \frac{\mu}{r_2^3} \right) = 0, \end{cases}$$

$$y=0, \begin{cases} x + \frac{1-\mu}{(x-\mu)^2} + \frac{\mu}{(x+1-\mu)^2} = 0, \\ x + \frac{1-\mu}{(x-\mu)^2} - \frac{\mu}{(x+1-\mu)^2} = 0, \\ x - \frac{1-\mu}{(x-\mu)^2} + \frac{\mu}{(x+1-\mu)^2} = 0, \end{cases}$$

$$y \neq 0, \begin{cases} 1 - \frac{1-\mu}{r_1^3} - \frac{\mu}{r_2^3} = 0, \\ x - \frac{(1-\mu)(x-\mu)}{r_1^3} - \frac{\mu(x+1-\mu)}{r_2^3} = 0. \end{cases}$$

$$\ddot{\mathbf{r}} + 2 \begin{pmatrix} -\dot{y} \\ \dot{x} \\ 0 \end{pmatrix} = \left(\frac{\partial \Omega}{\partial \mathbf{r}} \right)^T$$



平动点位置计算

$$\begin{cases} x - \frac{1-\mu}{(x+\mu)^2} + \frac{\mu}{(x-1+\mu)^2} = 0 \\ x - \frac{1-\mu}{(x+\mu)^2} - \frac{\mu}{(x-1+\mu)^2} = 0 \\ x + \frac{1-\mu}{(x+\mu)^2} + \frac{\mu}{(x-1+\mu)^2} = 0 \end{cases}$$

$$\begin{cases} 1 - \frac{1-\mu}{r_1^3} - \frac{\mu}{r_2^3} = 0 \\ x + \frac{(1-\mu)(x+\mu)}{r_1^3} - \frac{\mu(x-1+\mu)}{r_2^3} = 0 \end{cases}$$

$$\xi^{(1)} = \left(\frac{\mu}{3}\right)^{\frac{1}{3}} \left[1 - \frac{1}{3}\left(\frac{\mu}{3}\right)^{\frac{1}{3}} - \frac{1}{9}\left(\frac{\mu}{3}\right)^{\frac{2}{3}} + \dots\right],$$

$$\xi^{(2)} = \left(\frac{\mu}{3}\right)^{\frac{1}{3}} \left[1 + \frac{1}{3}\left(\frac{\mu}{3}\right)^{\frac{1}{3}} - \frac{1}{9}\left(\frac{\mu}{3}\right)^{\frac{2}{3}} - \dots\right],$$

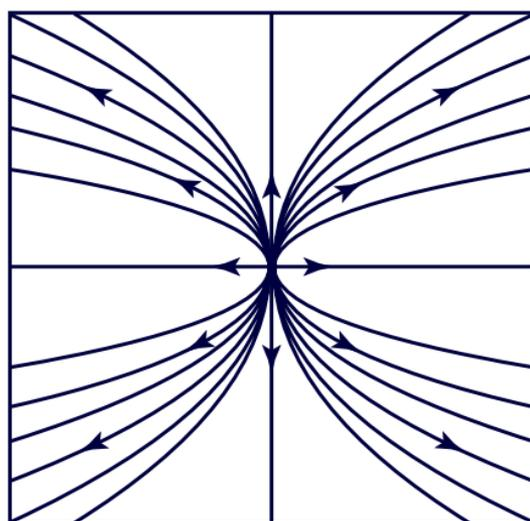
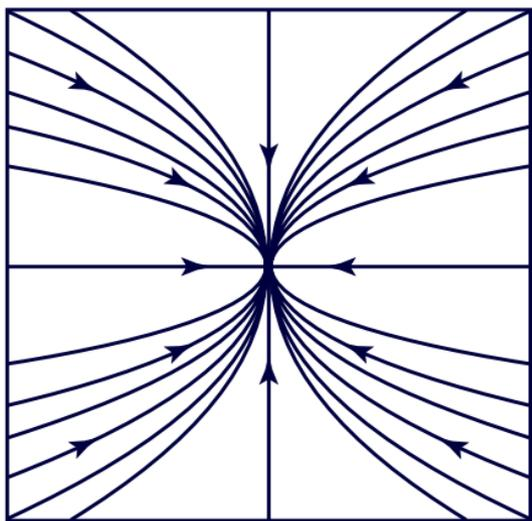
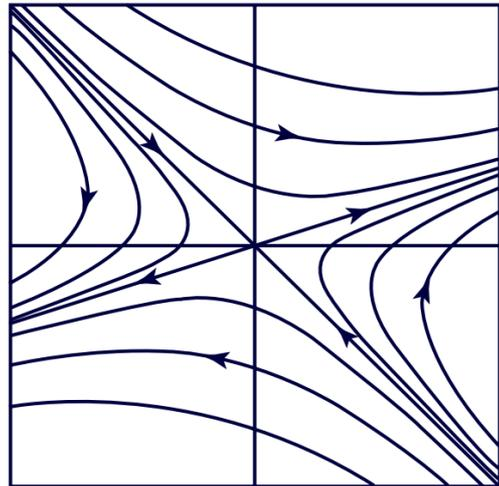
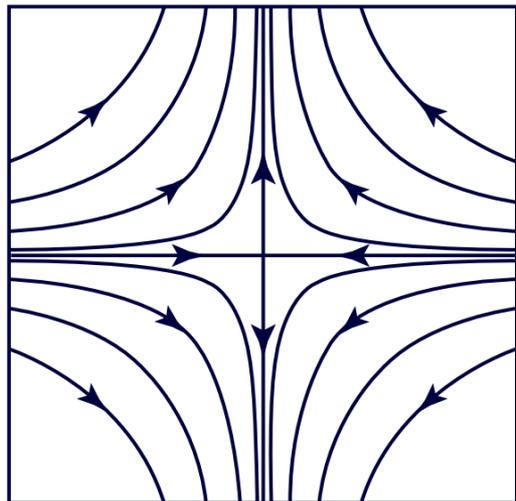
$$\begin{cases} \xi^{(3)} = 1 - \nu \left[1 + \frac{23}{84}\nu^2 + \frac{23}{84}\nu^3 + \frac{761}{2352}\nu^4 + \frac{3163}{7056}\nu^5 + \frac{30703}{49392}\nu^6\right] + O(\nu^8) \\ \nu = \frac{7}{12}\mu. \end{cases}$$

平面线性系统相异实特征根

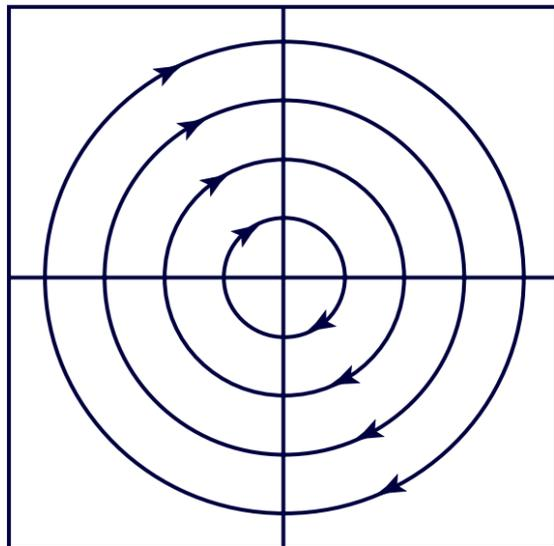
1. $\lambda_1 < 0 < \lambda_2$;
2. $\lambda_1 < \lambda_2 < 0$;
3. $0 < \lambda_1 < \lambda_2$.

鞍点相图

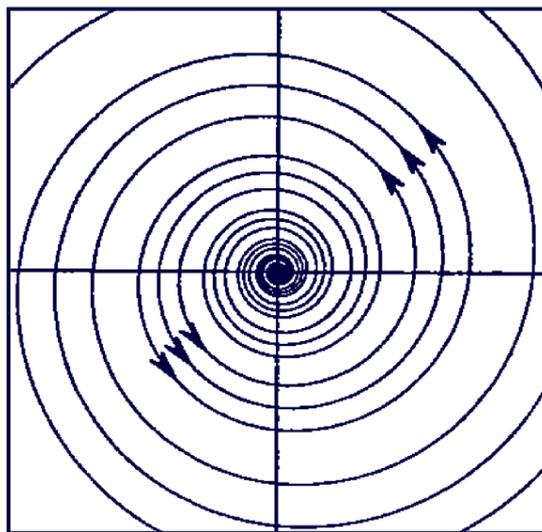
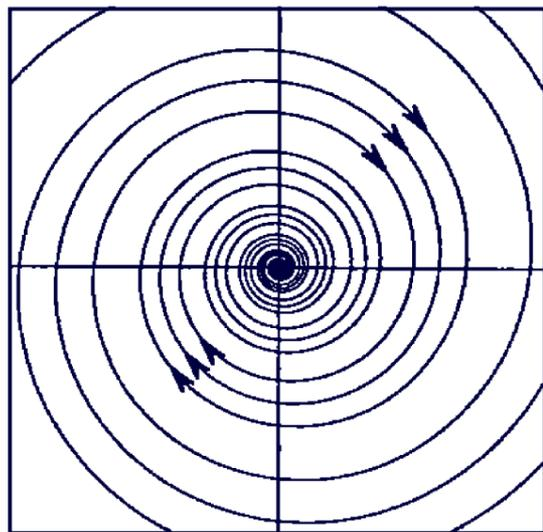
涵与源相图



平面线性系统复特征根



中心的相图



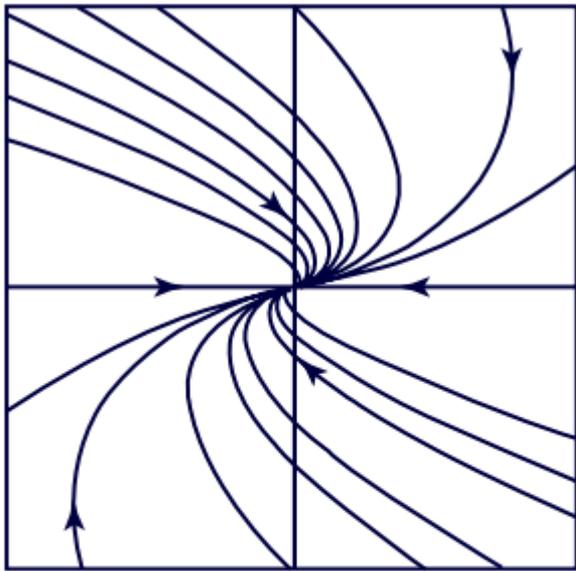
螺线涵和螺线源相图

重特征根与平面系统分类

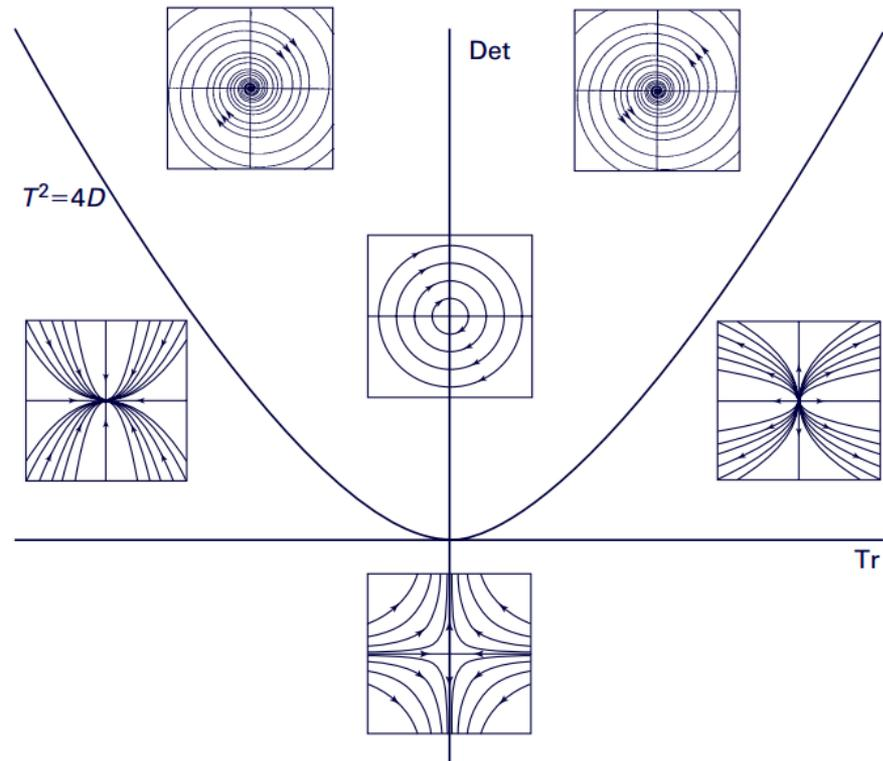
1. Complex with nonzero imaginary part if $T^2 - 4D < 0$;
2. Real and distinct if $T^2 - 4D > 0$;
3. Real and repeated if $T^2 - 4D = 0$

$$\frac{dx}{dt} = Ax$$

$$T = \text{tr } A \text{ and } D = \det A$$



Phase portrait for a system with repeated negative eigenvalues.

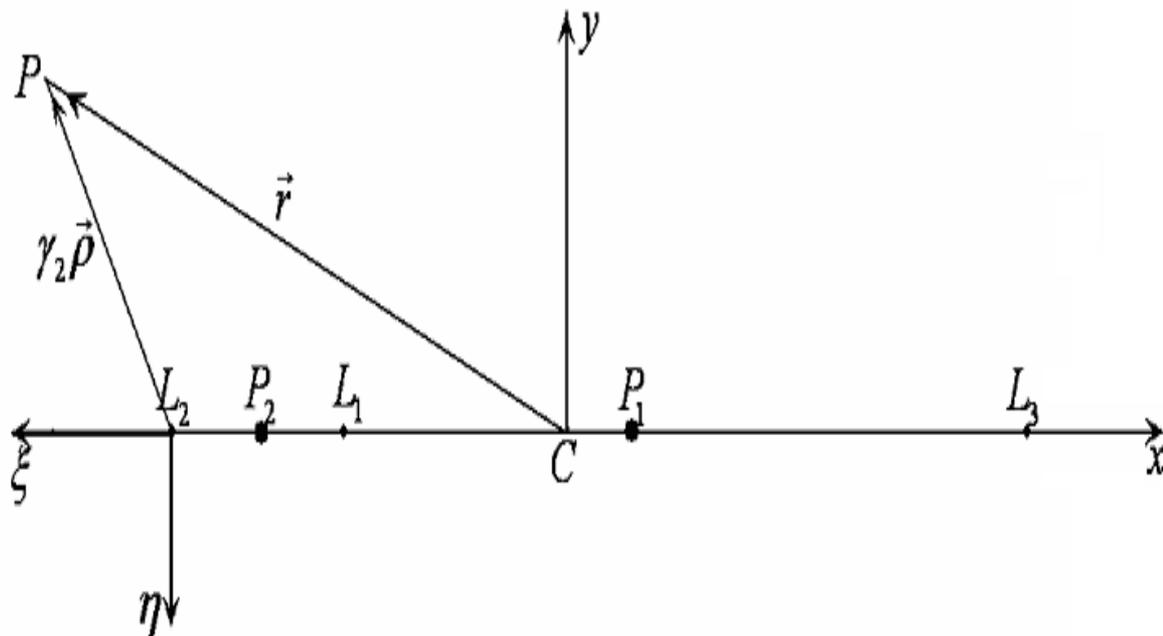


The trace-determinant plane. Any resemblance to any of the authors' faces is purely coincidental.

共线平动点动力学特征

会合坐标系无量纲运动方程

$$\begin{cases} \ddot{\vec{r}} + 2(-\dot{y}, \dot{x}, 0)^T = (\partial\Omega/\partial\vec{r})^T \\ \Omega(x, y, z) = (x^2 + y^2)/2 + (1-\mu)/r_1 + \mu/r_2 \end{cases}$$



共线平动点动力学特征

相对坐标系下方程

$$\frac{1}{\sqrt{(x-A)^2 + (y-B)^2 + (z-C)^2}} = \frac{1}{D} \sum_{n=0}^{\infty} \left(\frac{\rho}{D}\right)^n P_n\left(\frac{Ax + By + Cz}{D\rho}\right)$$

$$\begin{cases} \ddot{\xi} - 2\dot{\eta} - (1 + 2c_2)\xi = \partial/\partial\xi \left(\sum_{n \geq 3} c_n(\mu) \rho^n P_n(\xi/\rho) \right) \\ \dot{\eta} + 2\dot{\xi} - (1 - c_2)\eta = \partial/\partial\eta \left(\sum_{n \geq 3} c_n(\mu) \rho^n P_n(\xi/\rho) \right) \\ \ddot{\zeta} + c_2\zeta = \partial/\partial\zeta \left(\sum_{n \geq 3} c_n(\mu) \rho^n P_n(\xi/\rho) \right) \end{cases}$$

小天体相对共线平动点运动的线性化方程

$$\begin{cases} \ddot{\xi} - 2\dot{\eta} - (1 + 2c_2)\xi = 0 \\ \dot{\eta} + 2\dot{\xi} - (1 - c_2)\eta = 0 \\ \ddot{\zeta} + c_2\zeta = 0 \end{cases}$$

共线平动点动力学特征

齐次通解形式

$$\begin{cases} \xi = C_1 e^{d_1 t} + C_2 e^{-d_1 t} + C_3 \cos d_2 t + C_4 \sin d_2 t \\ \eta = \alpha_1 C_1 e^{d_1 t} - \alpha_1 C_2 e^{-d_1 t} - \alpha_2 C_3 \sin d_2 t + \alpha_2 C_4 \cos d_2 t \\ \zeta = C_5 \cos d_3 t + C_6 \sin d_3 t \end{cases}$$

$$\begin{cases} d_1 = \sqrt{(\sqrt{9c_2^2 - 8c_2} + c_2 - 2)}/2 \\ d_2 = \sqrt{(\sqrt{9c_2^2 - 8c_2} - c_2 + 2)}/2 \\ d_3 = \sqrt{c_2} \end{cases}$$

$$\alpha_1 = (d_1^2 - 2c_2 - 1)/2d_1 < 0,$$

$$\alpha_2 = (d_2^2 + 2c_2 + 1)/2d_2 > 0$$

从特征值可以看到共线平动点是不稳定的。

三个特征值分别为 $\pm d_1, \pm id_2, \pm id_3$ $\pm id_2, \pm id_3$ 存在表明共线平动点附近存在中心流形（即周期或拟周期轨道），通常称这些中心流形为条件稳定轨道。

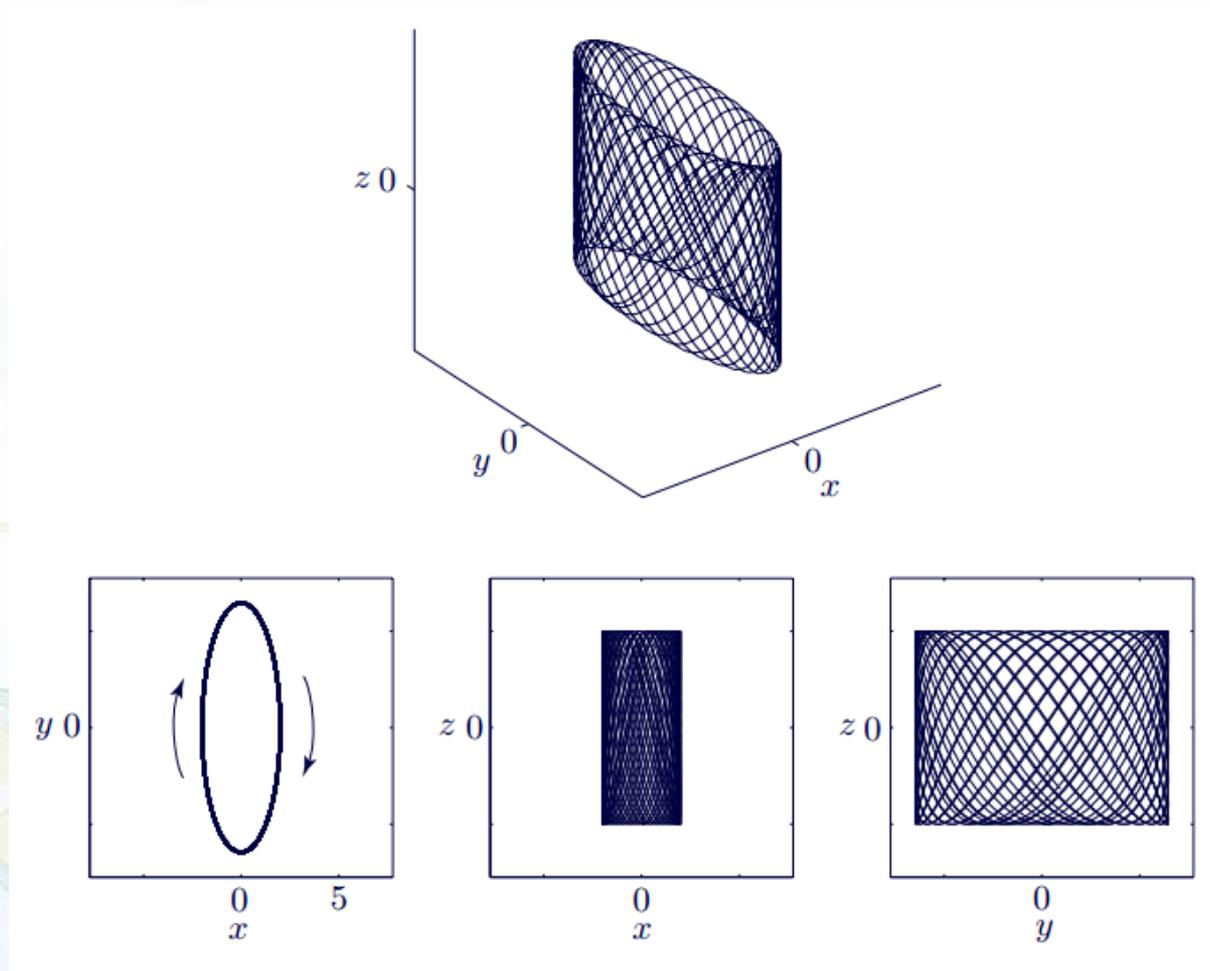
条件稳定解

若选取如下初始条件即可使 $C_1 = C_2 = 0$

$$\begin{cases} \xi(t) = \alpha \mathbf{cos}(\omega_0 t + \phi_1) \\ \eta(t) = \kappa \alpha \mathbf{sin}(\omega_0 t + \phi_1) \\ \zeta(t) = \beta \mathbf{cos}(\nu_0 t + \phi_2) \end{cases}$$

ω_0 ν_0 一般不通约，以上方程表示一拟周期轨道，称为Lissajous轨道。

Lissajous轨道



考虑高次扰动解

线性化模型下的条件稳定轨道在考虑高次项扰动后仍然存在，有如下形式

$$\left\{ \begin{array}{l} \xi(t) = \sum_{i,j=1}^{\infty} \left(\sum_{|k|\leq i, |m|\leq j} \xi_{ijkm} \cos(k\theta_1 + m\theta_2) \right) \alpha^i \beta^j \\ \eta(t) = \sum_{i,j=1}^{\infty} \left(\sum_{|k|\leq i, |m|\leq j} \eta_{ijkm} \sin(k\theta_1 + m\theta_2) \right) \alpha^i \beta^j \\ \zeta(t) = \sum_{i,j=1}^{\infty} \left(\sum_{|k|\leq i, |m|\leq j} \zeta_{ijkm} \cos(k\theta_1 + m\theta_2) \right) \alpha^i \beta^j \end{array} \right.$$

$$\theta_1 = \omega t + \phi_1, \theta_2 = \nu t + \phi_2$$

Halo轨道

虽然， ω_0 与 μ_0 不等。但非线性项的扰动会使 ω 与 μ ，此时拟周期轨道变为周期轨道，这种周期轨道称为晕（halo）轨道

$$\begin{cases} x(t) = \sum_{i,j=1}^{\infty} \left(\sum_{|k| \leq i+j} x_{ijk} \cos(k\theta) \right) \alpha^i \beta^j \\ y(t) = \sum_{i,j=1}^{\infty} \left(\sum_{|k| \leq i+j} y_{ijk} \sin(k\theta) \right) \alpha^i \beta^j \\ z(t) = \sum_{i,j=1}^{\infty} \left(\sum_{|k| \leq i+j} z_{ijk} \cos(k\theta) \right) \alpha^i \beta^j \end{cases}$$

$$\theta = \omega t + \phi$$

Halo轨道三阶解析解（Poincare-Lindstedt方法） by Richardson

$$\begin{aligned}
 x &= a_{21}A_x^2 + a_{22}A_z^2 - A_x \cos \tau_1 \\
 &\quad + (a_{23}A_x^2 - a_{24}A_z^2) \cos 2\tau_1 + (a_{31}A_x^3 - a_{32}A_xA_z^2) \cos 3\tau_1, \\
 y &= \kappa A_x \sin \tau_1 \\
 &\quad + (b_{21}A_x^2 - b_{22}A_z^2) \sin 2\tau_1 + (b_{31}A_x^3 - b_{32}A_xA_z^2) \sin 3\tau_1, \\
 z &= \delta_m A_z \cos \tau_1 \\
 &\quad + \delta_m d_{21}A_xA_z(\cos 2\tau_1 - 3) + \delta_m(d_{32}A_zA_x^2 - d_{31}A_z^3) \cos 3\tau_1.
 \end{aligned}$$

$$a_{21} = \frac{3c_3(\kappa^2 - 2)}{4(1 + 2c_2)},$$

$$a_{22} = \frac{3c_3}{4(1 + 2c_2)},$$

$$a_{23} = -\frac{3c_3\omega_p}{4\kappa d_1} (3\kappa^3\omega_p - 6\kappa(\kappa - \omega_p) + 4)$$

$$a_{24} = -\frac{3c_3\omega_p}{4\kappa d_1} (2 + 3\kappa\omega_p),$$

$$b_{21} = -\frac{3c_3\omega_p}{2d_1} (3\kappa\omega_p - 4),$$

$$b_{22} = -\frac{3c_3\omega_p}{d_1},$$

$$d_{21} = -\frac{c_3}{2\omega_p^2},$$

$$\begin{aligned}
 a_{31} &= -\frac{9\omega_p}{4d_2} (4c_3(\kappa a_{23} - b_{21}) + \kappa c_4(4 + \kappa^2)) \\
 &\quad + \frac{9\omega_p^2 + 1 - c_2}{2d_2} (3c_3(2a_{23} - \kappa b_{21}) + c_4(2 + 3\kappa^2))
 \end{aligned}$$

$$\begin{aligned}
 a_{32} &= -\frac{9\omega_p}{4d_2} (4c_3(3\kappa a_{24} - b_{22}) + \kappa c_4) \\
 &\quad - \frac{3}{2d_2} (9\omega_p^2 + 1 - c_2) (c_3(\kappa b_{22} + d_{21} - 2a_{24}) - c_4)
 \end{aligned}$$

Halo轨道Richardson三阶解析解

$$b_{31} = \frac{3}{8d_2} 8\omega_p (3c_3(\kappa b_{21} - 2a_{23}) - c_4(2 + 3\kappa^2)) \\ + \frac{3}{8d_2} ((9\omega_p^2 + 1 + 2c_2)(4c_3(\kappa a_{23} - b_{21}) + \kappa c_4(4 + \kappa^2)),$$

$$b_{32} = \frac{9\omega_p}{d_2} (c_3(\kappa b_{22} + d_{21} - 2a_{24}) - c_4) \\ + \frac{3(9\omega_p^2 + 1 + 2c_2)}{8d_2} (4c_3(\kappa a_{24} - b_{22}) + \kappa c_4),$$

$$d_{31} = \frac{3}{64\omega_p^2} (4c_3 a_{24} + c_4),$$

$$d_{32} = \frac{3}{64\omega_p^2} (4c_3(a_{23} - d_{21}) + c_4(4 + \kappa^2)),$$

$$s_1 = (2\omega_p(\omega_p(1 + \kappa^2) - 2\kappa))^{-1} \\ \times \left(\frac{3}{2}c_3(2a_{21}(\kappa^2 - 2) - a_{23}(\kappa^2 + 2) - 2\kappa b_{21}) - \frac{3}{8}c_4(3\kappa^4 - 8\kappa^2 + 8) \right),$$

$$s_2 = (2\omega_p(\omega_p(1 + \kappa^2) - 2\kappa))^{-1} \\ \times \left(\frac{3}{2}c_3(2a_{22}(\kappa^2 - 2) + a_{24}(\kappa^2 + 2) + 2\kappa b_{22} + 5d_{21}) + \frac{3}{8}c_4(12 - \kappa^2) \right)$$

$$l_1 = -\frac{3}{2}c_3(2a_{21} + a_{23} + 5d_{21}) - \frac{3}{8}c_4(12 - \kappa^2) + 2\omega_p^2 s_1,$$

$$l_2 = \frac{3}{2}c_3(a_{24} - 2a_{22}) + \frac{9}{8}c_4 + 2\omega_p^2 s_2,$$

数值法改正

$$\begin{aligned}\dot{\bar{x}} &= f(\bar{x}), \\ \dot{\Phi}(t, t_0) &= Df(\bar{x})\Phi(t, t_0),\end{aligned}$$

$$\mathcal{U} = \begin{pmatrix} \bar{U}_{xx} & \bar{U}_{xy} & \bar{U}_{xz} \\ \bar{U}_{yx} & \bar{U}_{yy} & \bar{U}_{yz} \\ \bar{U}_{zx} & \bar{U}_{zy} & \bar{U}_{zz} \end{pmatrix}$$

$$\begin{aligned}\bar{x}(t_0) &= \bar{x}_0, \\ \Phi(t_0, t_0) &= I_6.\end{aligned}$$

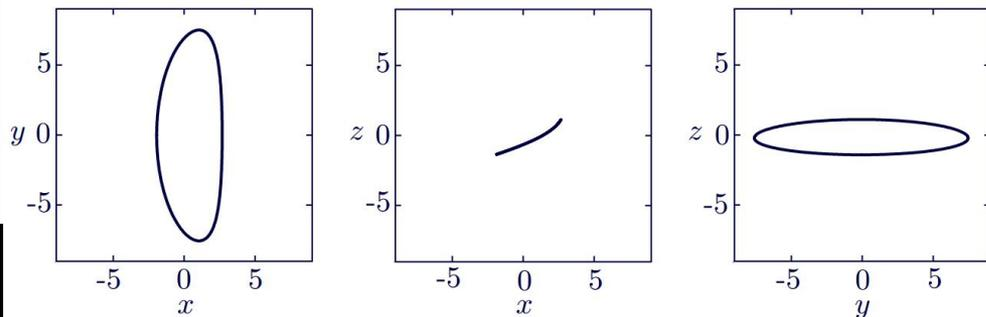
$$Df(\bar{x}) = \begin{pmatrix} 0 & I_3 \\ -\mathcal{U} & 2\Omega \end{pmatrix}$$

$$\bar{x}_0 = (x_0, 0, z_0, 0, \dot{y}_0, 0)^T.$$

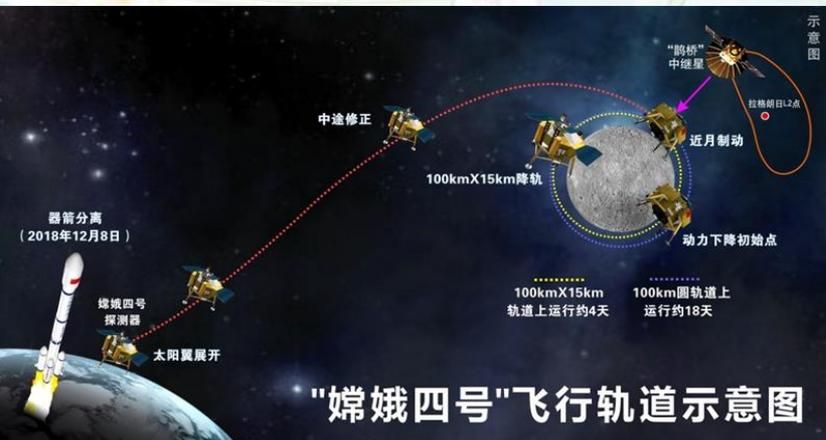
$$\bar{x}_f = (x_f, 0, z_f, 0, \dot{y}_f, 0)^T$$

$$\Omega = \begin{pmatrix} 0 & 1 & 0 \\ -1 & 0 & 0 \\ 0 & 0 & 0 \end{pmatrix}$$

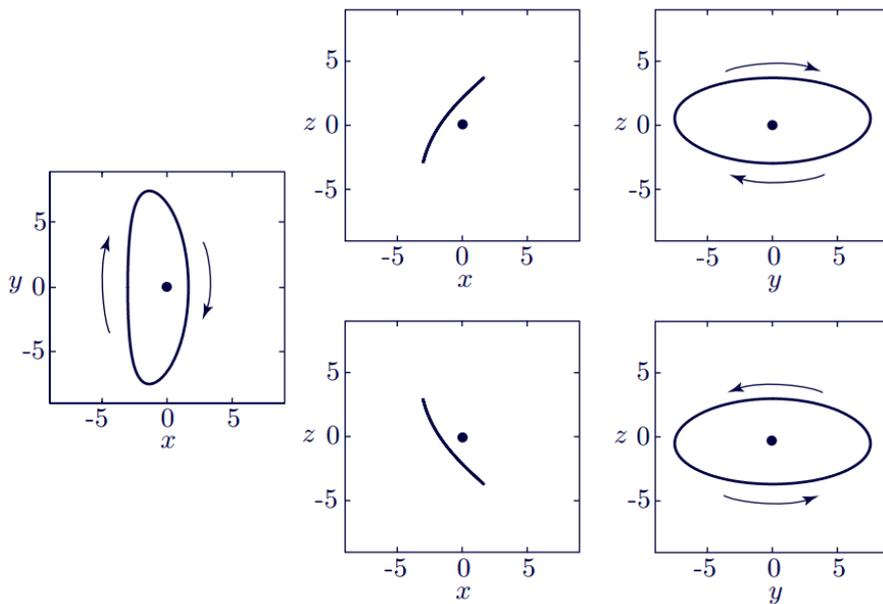
Halo轨道



The halo orbit used by the ISEE-3 mission. From left to right, the xy , xz , and yz projections are shown. The Sun-Earth L_1 point is the origin, with coordinate values given in increments of 10^5 km.



"嫦娥四号"飞行轨道示意图



A northern halo (top) and southern halo (bottom) about the Sun-Earth L_2 . From left to right, the xy , xz , and yz projections are shown. The xy projections are the same. Arrows indicate the direction of motion in the xy and yz projections. The Sun-Earth L_2 point is the dot at the origin. Coordinate values are given in increments of 10^5 km. $|A_z|=330,000$ km for both halos.

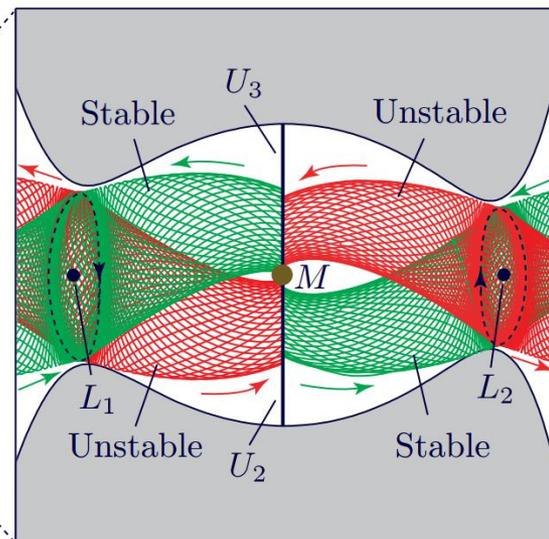
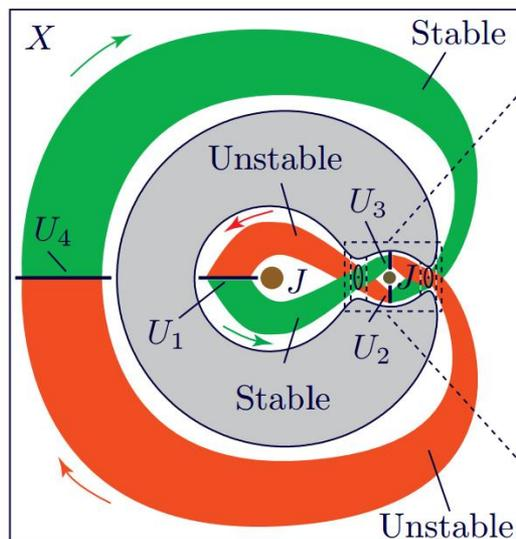
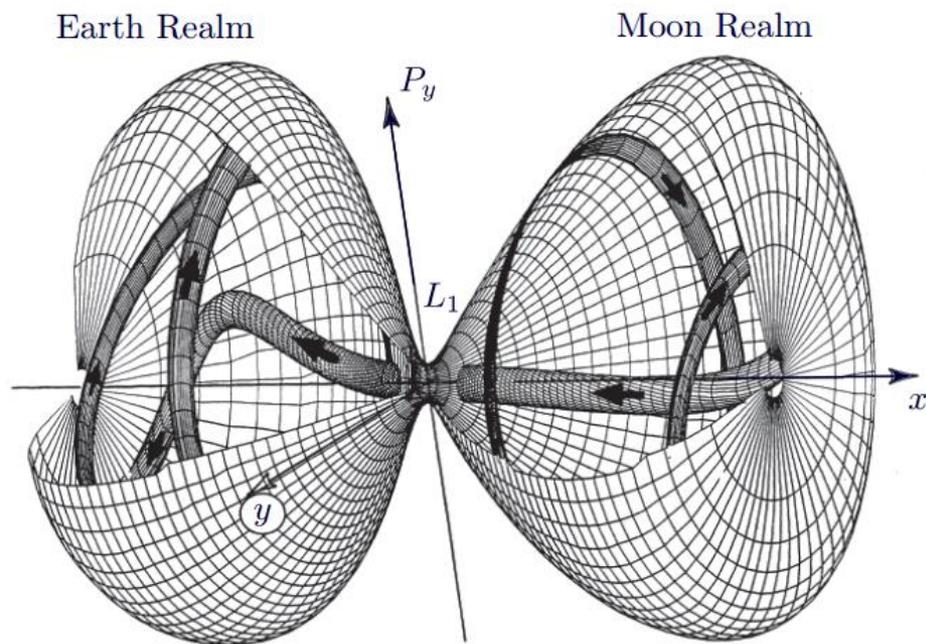
共线平动点应用

● 定点探测器

由于在太阳系真实引力模型下存在各种摄动（这些摄动主要来自系统外其它大天体和两个主天体的轨道偏心率），这些摄动的频率往往不公约，因此实际上周期轨道是不存在的，能存在的仅是拟周期轨道（拟晕轨道或者Lissajous轨道）。

● 节能过渡

共线平动点附近的稳定与不稳定流形构成了一些节能不走走廊，探测器可以通过这些走廊无动力地从共线平动点的一侧穿越到另一侧，该动力学特征为发射深空探测器提供了一种节能途径。



三角平动点稳定性分析

The coordinates of the point L_4 are $\xi = \frac{1}{2}(1 - 2\mu)$ and $\eta = \sqrt{3}/2$, so that the linearised equations of motion are

$$\begin{aligned}\ddot{x} - 2\dot{y} &= \frac{3}{4}x + \frac{3\sqrt{3}}{4}(1 - 2\mu)y, \\ \ddot{y} + 2\dot{x} &= \frac{9}{4}y + \frac{3\sqrt{3}}{4}(1 - 2\mu)x.\end{aligned}$$

Substitution of the trial solution gives

$$\omega^4 + \omega^2 + \frac{27}{4}\mu(1 - \mu) = 0.$$

Because

$$\omega_1^2 \omega_2^2 = \frac{27}{4}\mu(1 - \mu) > 0,$$

the possible real roots have the same sign. Since also

$$\omega_1^2 + \omega_2^2 = -1 < 0,$$

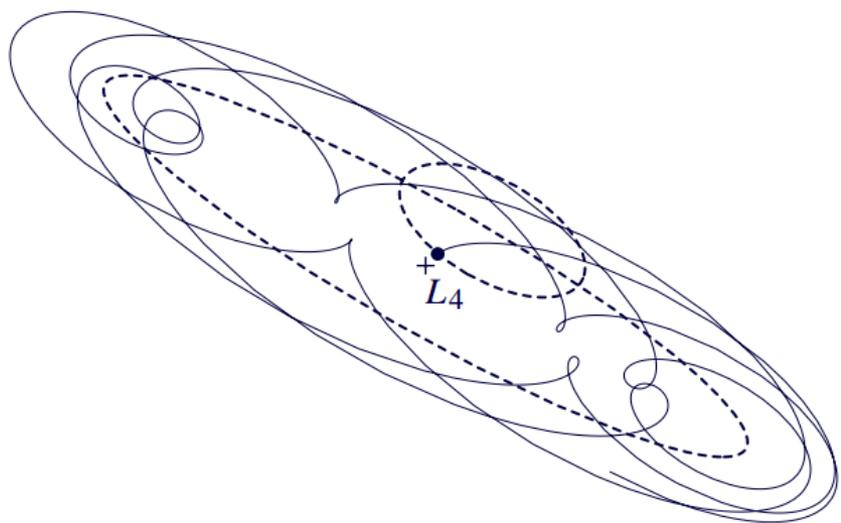
both roots ω_i^2 must be negative.

三角平动点动力学特征

线性意义下稳定条件

$$0 < \mu < \mu_0 = \frac{1}{2} \left(1 - \sqrt{\frac{69}{9}} \right) = 0.038520896504551L$$

在太阳系中如日—木—小行星，日—地—月球，以及地—月—探测器等均满足。



在限制性三体问题模型下，地—月系中三角平动点附近定位的探测器有一定初值误差时，可长期保持在其周围，而日—地系中三角平动点附近的探测器将会在大范围内漂移。

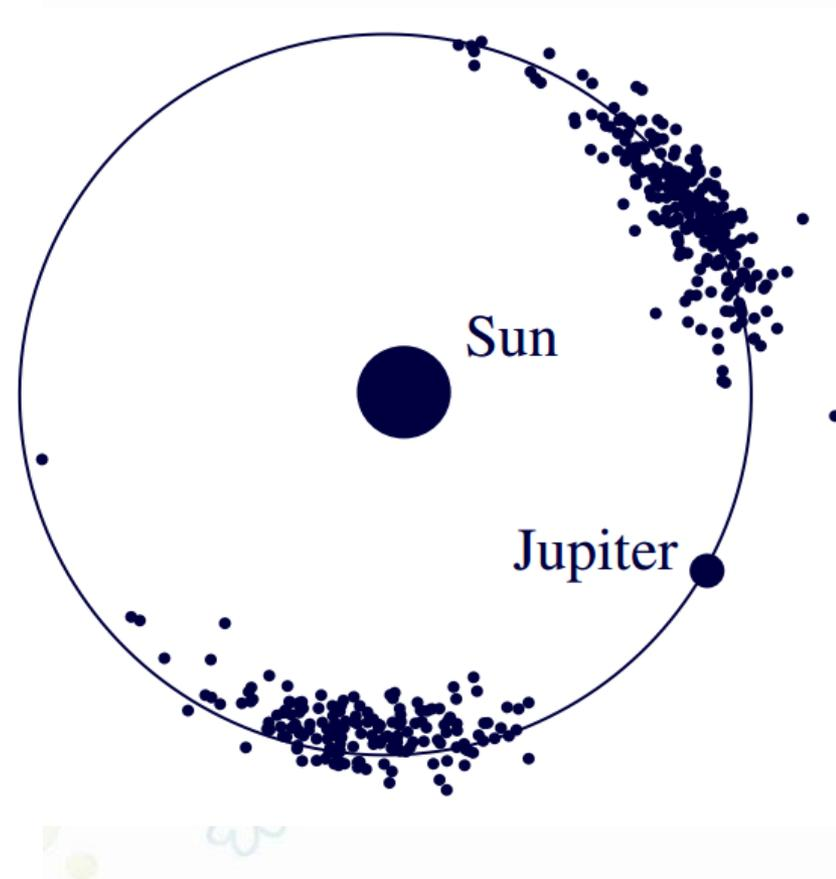
考虑其它天体引力影响时，对地—月—探测器系统，由于摄动量级较大，这将会改变稳定性状态，最终导致定位在地—月系三角平动点附近的探测器发生明显的位置漂移并远离而去。

若考虑发射这类探测器，即使三角平动点是稳定的，仍旧需要在其工作寿命期间进行相应的轨控。

日-木系统Trojan小行星

Orbital properties of the Trojan asteroids with numbers less than 2,000 that are associated with the Sun-Jupiter system. D is the amplitude of libration; e_{pr} and I_{pr} are the proper eccentricity and inclination respectively as determined by Milani (1993). The final entry indicates whether libration takes place about the L_4 or L_5 point.

Asteroid	D ($^{\circ}$)	e_{pr}	$\sin I_{pr}$	L_4	L_5
(588) Achilles	6.45	0.1032	0.1967	•	
(617) Patroclus	5.02	0.1005	0.3662		•
(624) Hektor	18.99	0.0543	0.3259	•	
(659) Nestor	10.03	0.1297	0.0870	•	
(884) Priamus	10.82	0.0883	0.1739		•
(911) Agamemnon	16.95	0.0207	0.3857	•	
(1143) Odysseus	9.84	0.0521	0.0689	•	
(1172) Aeneas	10.15	0.0602	0.3056		•
(1173) Anchises	23.99	0.0914	0.1404	•	
(1208) Troilus	10.63	0.0354	0.5446	•	
(1404) Ajax	19.98	0.0761	0.3270	•	
(1437) Diomedes	28.73	0.0179	0.3653	•	
(1583) Antilochus	24.36	0.0183	0.4858	•	
(1647) Menelaus	7.93	0.0587	0.1168	•	
(1749) Telamon	13.61	0.0686	0.1185	•	
(1867) Deiphobus	17.50	0.0294	0.4738		•
(1868) Thersites	22.88	0.0979	0.2906	•	
(1869) Philoctetes	21.04	0.0576	0.0596	•	
(1870) Glaukos	9.49	0.0169	0.1114		•
(1871) Astyanax	27.76	0.0142	0.1299	•	
(1872) Helenos	23.55	0.0148	0.2538	•	
(1873) Agenor	12.08	0.1168	0.3791	•	



Hill限制性三体问题

$$\begin{cases} \ddot{\xi} = 2\dot{\eta} + \xi - \frac{\mu\xi}{(\xi^2 + \eta^2 + \zeta^2)^{\frac{3}{2}}} - \frac{(1-\mu)(\xi+1)}{((\xi+1)^2 + \eta^2 + \zeta^2)^{\frac{3}{2}}} + 1 - \mu \\ \ddot{\eta} = -2\dot{\xi} + \eta - \frac{\mu\eta}{(\xi^2 + \eta^2 + \zeta^2)^{\frac{3}{2}}} - \frac{(1-\mu)\eta}{((\xi+1)^2 + \eta^2 + \zeta^2)^{\frac{3}{2}}} \\ \ddot{\zeta} = -\frac{\mu\zeta}{(\xi^2 + \eta^2 + \zeta^2)^{\frac{3}{2}}} - \frac{(1-\mu)\zeta}{((\xi+1)^2 + \eta^2 + \zeta^2)^{\frac{3}{2}}} \end{cases}$$

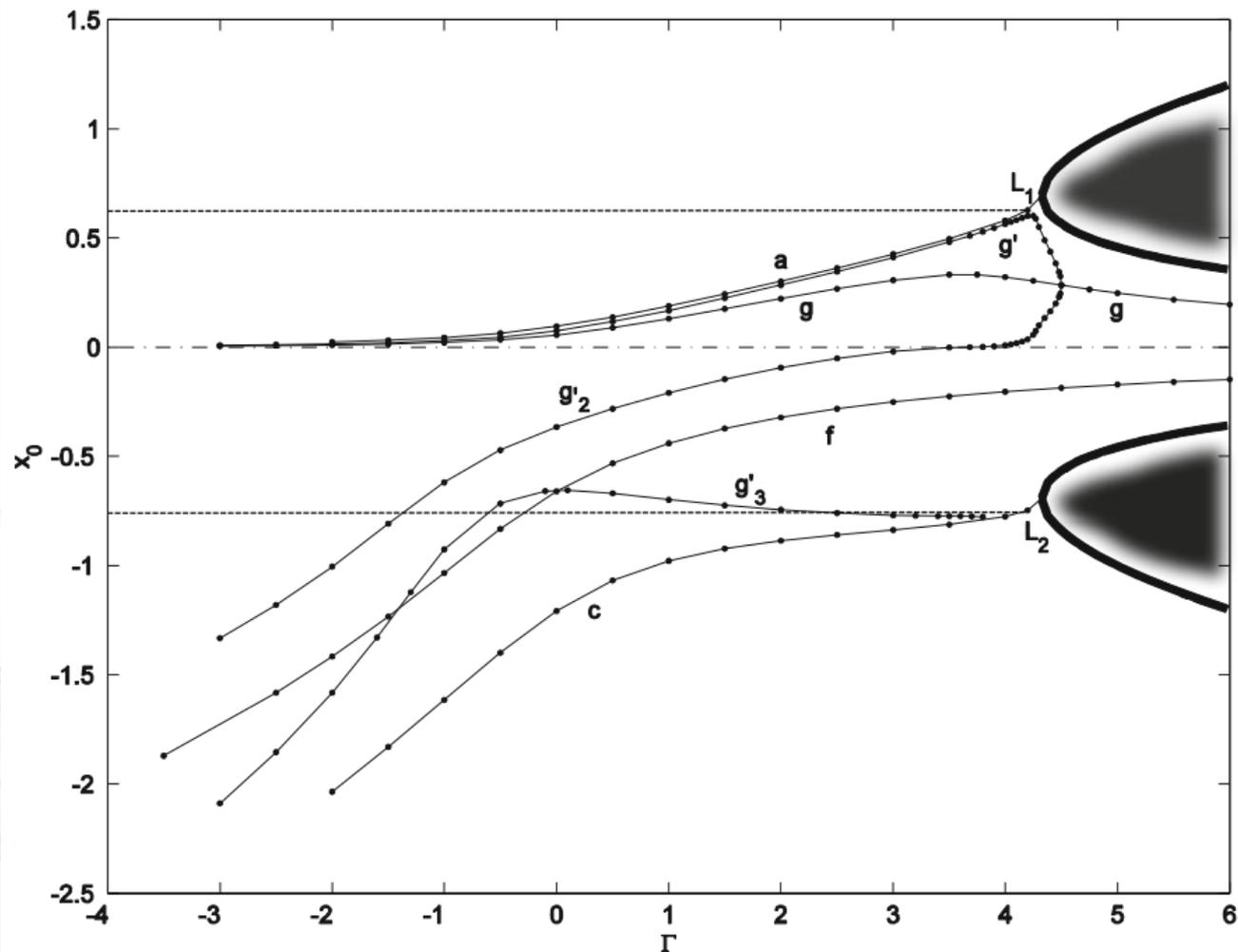
$$\begin{cases} \ddot{x} - 2\dot{y} - 3x = \frac{\partial W}{\partial x} \\ \ddot{y} + 2\dot{x} = \frac{\partial W}{\partial y} \\ \ddot{z} + z = \frac{\partial W}{\partial z} \end{cases}$$

$$W \equiv \frac{1}{r} = \frac{1}{\sqrt{x^2 + y^2 + z^2}}$$

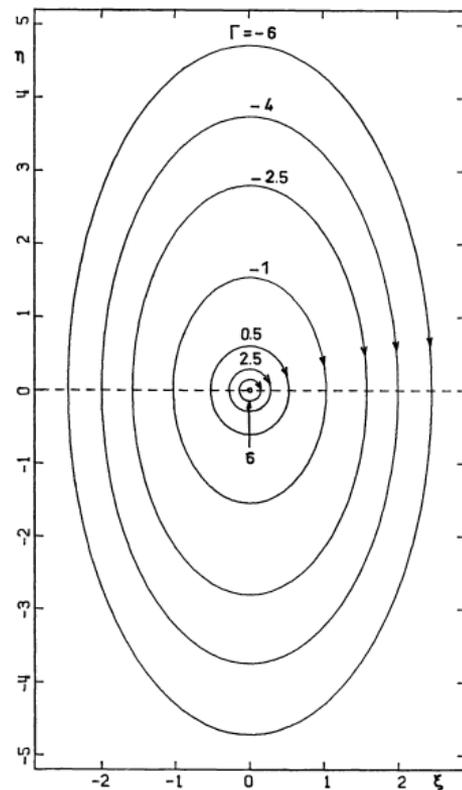
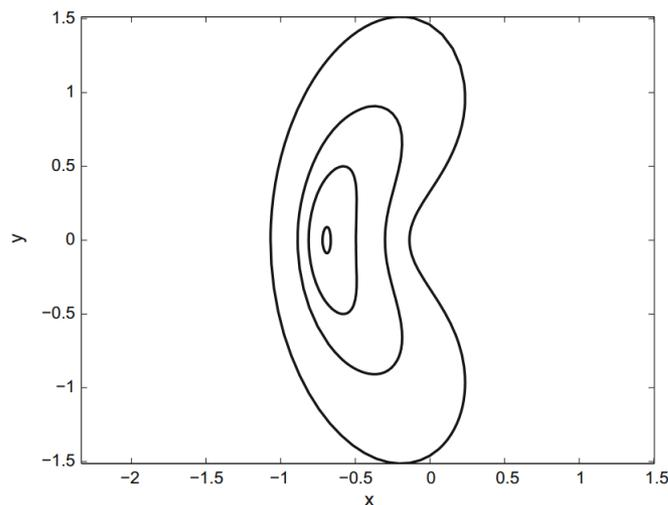
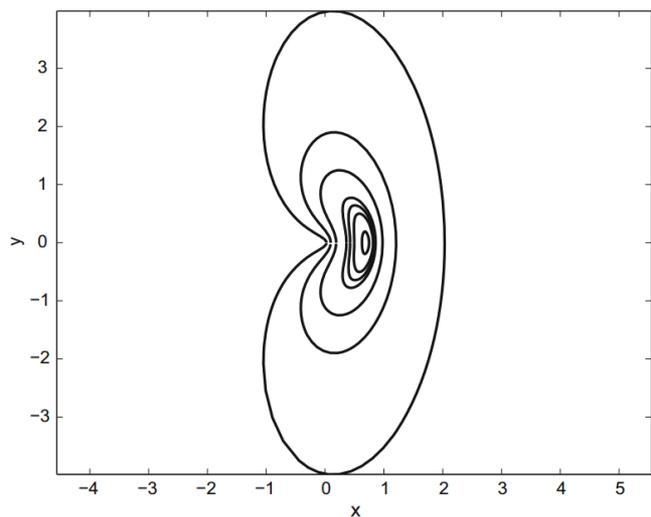
$$\Gamma = 3x^2 + z^2 + \frac{2}{r} - (\dot{x}^2 + \dot{y}^2 + \dot{z}^2)$$

$$L_3 \rightarrow -\infty, (L_1, L_2) = \pm \left(\frac{1}{3}\right)^{\frac{1}{3}} \approx 0.69336$$

Hill限制性三体问题周期轨道



周期轨道族 (a,c,f)



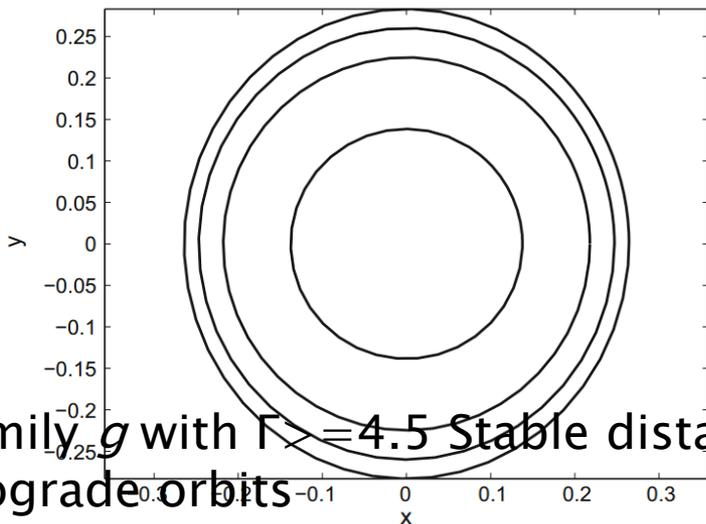
Family a in Hill's problem

Family c in Hill's problem

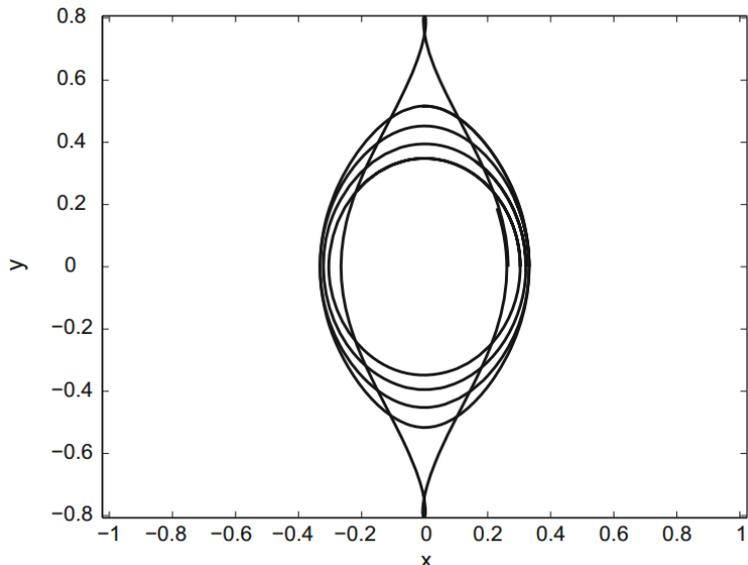
Family f in Hill's problem

a,c族周期轨道包括共线平动点L1,L2

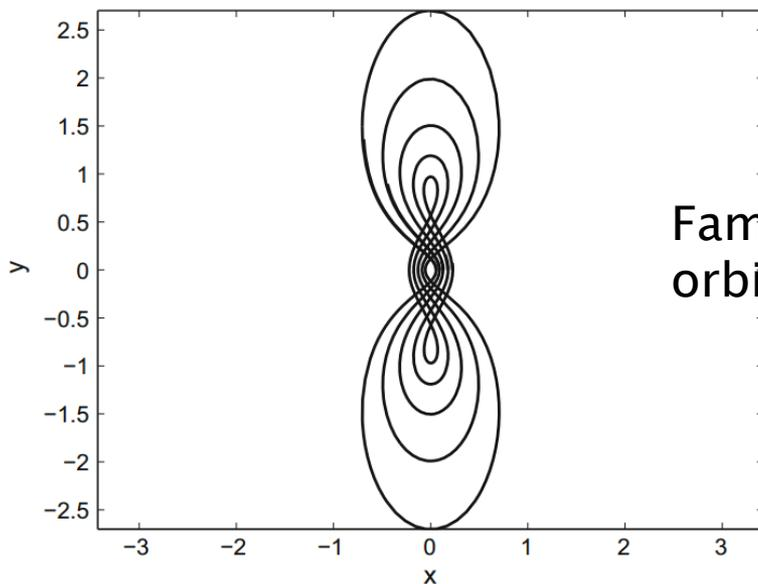
周期轨道族 (g)



Family g with $\Gamma \geq 4.5$ Stable distant prograde orbits



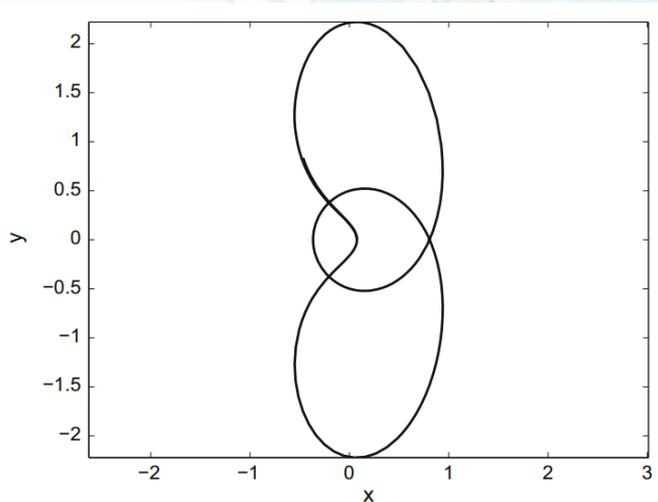
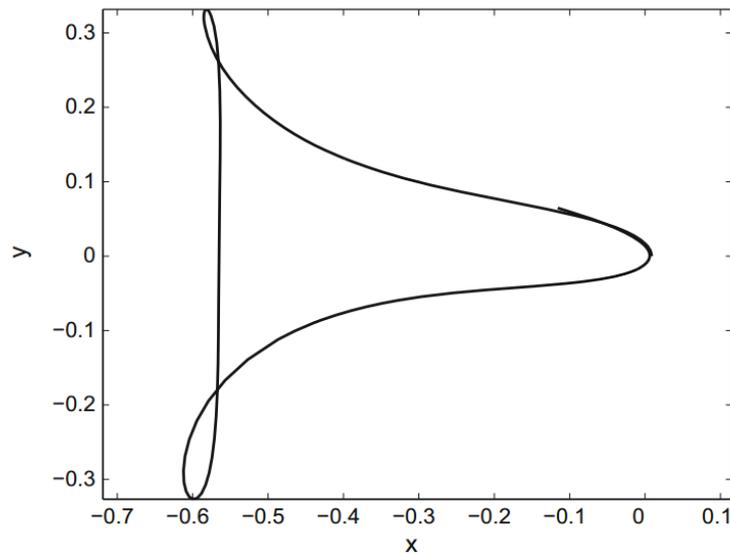
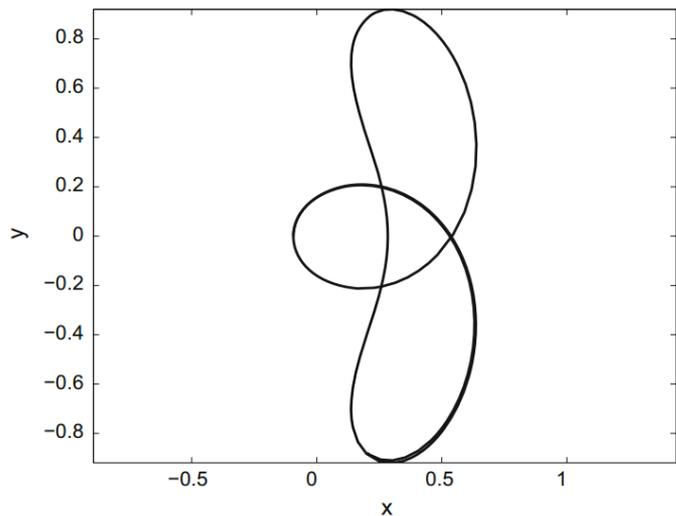
Family g with $2 \leq \Gamma \leq 4.5$ Unstable prograde orbits



Family g with $\Gamma < 2$: Unstable prograde orbits

WIND任务中利用不稳定性, 进行轨道转移。 NASA研制的日地空间探测卫星, 该卫星由美国全球近地空间科学计划发起, 并加入了国际日地空间物理学计划, 该任务的目标是研究太阳风中高能粒子的起源, 加速机制和传播过程。调查太阳风的质量和动量, WIND卫星经过2次月球借力飞行的转移轨道前往日地系统L1点的halo轨道

周期轨道族 (g')

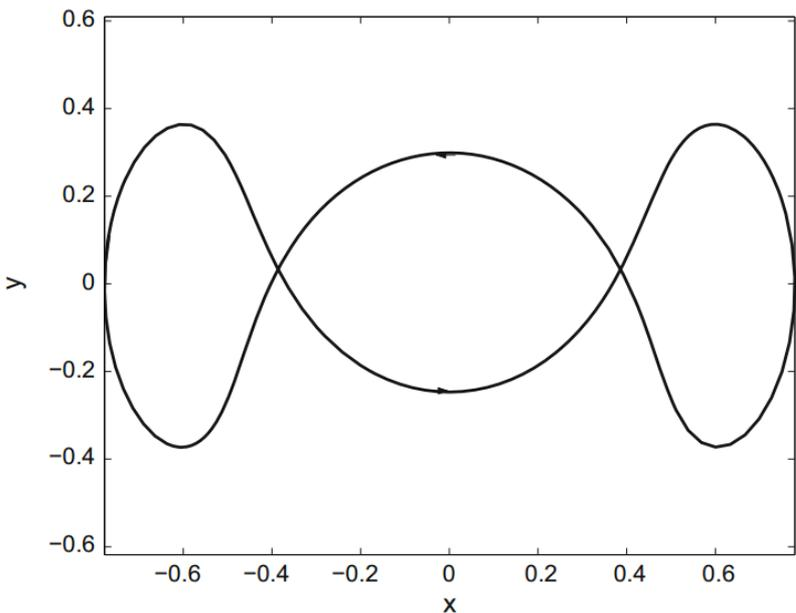


Family g' : Unstable orbits

g' 族第二类轨道接近于双曲线飞掠地球。图9是一种“弹弓”效果，一个飞船被转移到相对于一颗行星的逃逸轨道效应。

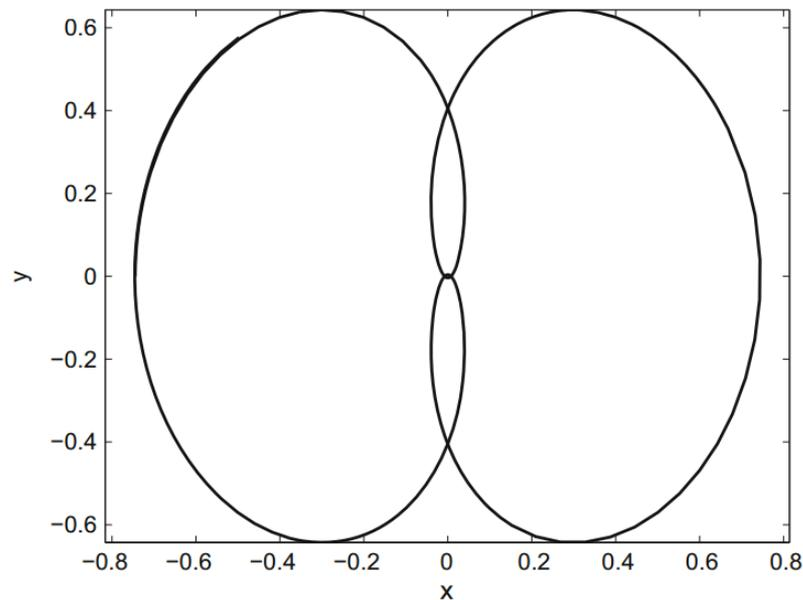
Family g' : Delayed escape

周期轨道族(g3)



Family g_3 : Libration point transfer

这种轨道在飞行过程中会接近平动点附近，并且可以作为平动点之间的转移轨道。



Family g_3 : Libration point and planet orbiter

这种轨道会经过次质量大天体附近和平动点附近，这种特征可以用来进行行星和共线平动点的转移运输轨道，因为需要的能量较小，且机动次数较少。

构造相流函数进行轨道搜索

$$L(x, y, z, \dot{x}, \dot{y}, \dot{z}) = \frac{1}{2} \left[(\dot{x} - y)^2 + (\dot{y} + x)^2 + \dot{z}^2 \right] - U(x, y, z)$$

$$U(x, y, z) = -\frac{\mu_1}{r_1} - \frac{\mu_2}{r_2} - \frac{1}{2} \mu_1 \mu_2$$

初始条件 x_0, Γ $\mathbf{X}_0 = [x_0, 0, 0, \dot{y}(\Gamma, x_0)]$

$$H = \frac{1}{2} \left[(p_x + y)^2 + (p_y - x)^2 + p_z^2 \right] + \tilde{U}$$

搜索目标 $\mathbf{X}_t^* = [x_0, 0, 0, \dot{y}(\Gamma, x_0)]$

$$\tilde{U} = -\frac{1}{2} (x^2 + y^2) + U$$

周期轨道（闭轨）相流非线性方程

第一变分方程

$$\frac{d\Phi}{dt} = \mathbf{A}\Phi$$

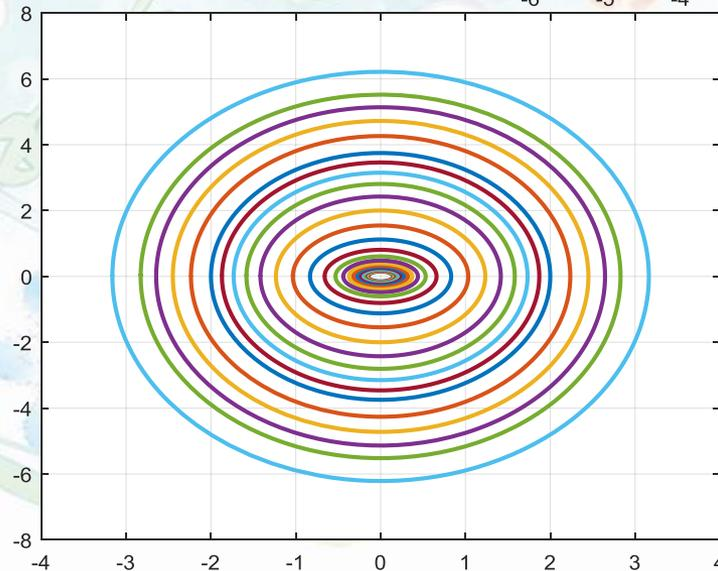
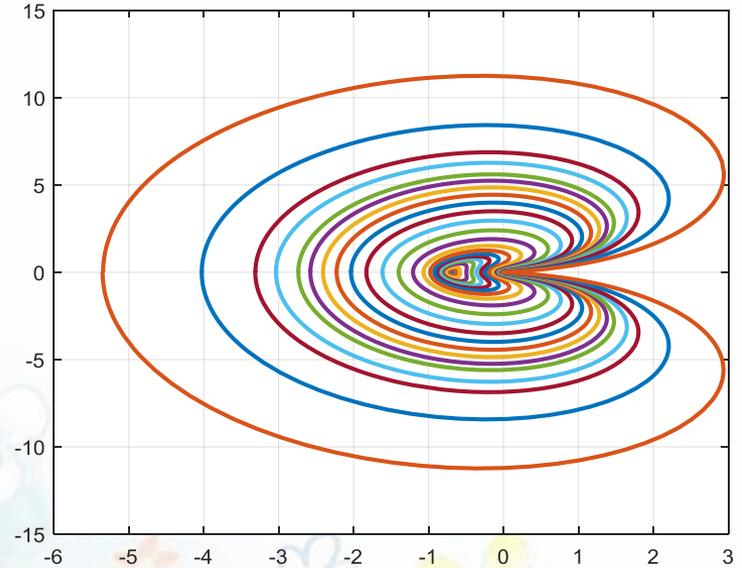
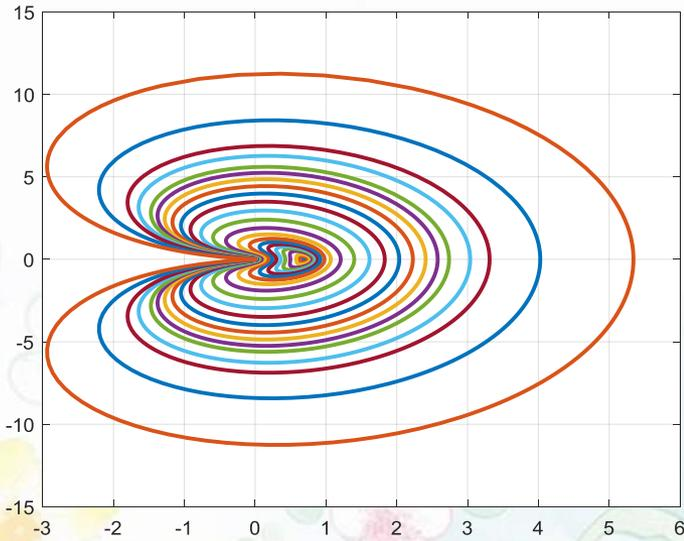
$$\mathbf{G}(\mathbf{X}) \stackrel{\text{def}}{=} \begin{bmatrix} \varphi_x(x_0, 0, 0, \dot{y}_0, \tau) - x_0 \\ \varphi_y(x_0, 0, 0, \dot{y}_0, \tau) \\ \varphi_{\dot{x}}(x_0, 0, 0, \dot{y}_0, \tau) \end{bmatrix} = \begin{bmatrix} 0 \\ 0 \\ 0 \end{bmatrix}$$

$$\mathbf{A} = \begin{bmatrix} 0 & 0 & 1 & 0 \\ 0 & 0 & 0 & 1 \\ \frac{\partial F_3}{\partial x} & \frac{\partial F_3}{\partial y} & 0 & 2 \\ \frac{\partial F_4}{\partial x} & \frac{\partial F_4}{\partial y} & -2 & 0 \end{bmatrix}$$

$$-\mathbf{G}(\mathbf{X}) = \frac{\partial \mathbf{G}}{\partial [x, \tau]} \Delta \begin{bmatrix} x \\ \tau \end{bmatrix}$$

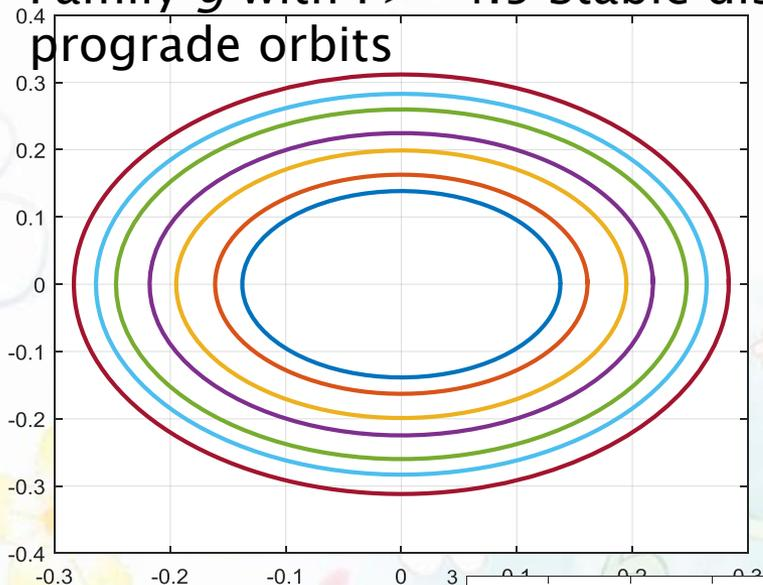
$$\frac{\partial \mathbf{G}}{\partial \begin{bmatrix} x \\ \tau \end{bmatrix}^T} = \begin{bmatrix} \frac{\partial \varphi_x}{\partial x} - 1 & \dot{x} \\ \frac{\partial \varphi_y}{\partial x} & \dot{y} \\ \frac{\partial \varphi_{v_x}}{\partial x} & f_3 \end{bmatrix}$$

自编软件搜索轨道 (a,c,f族)

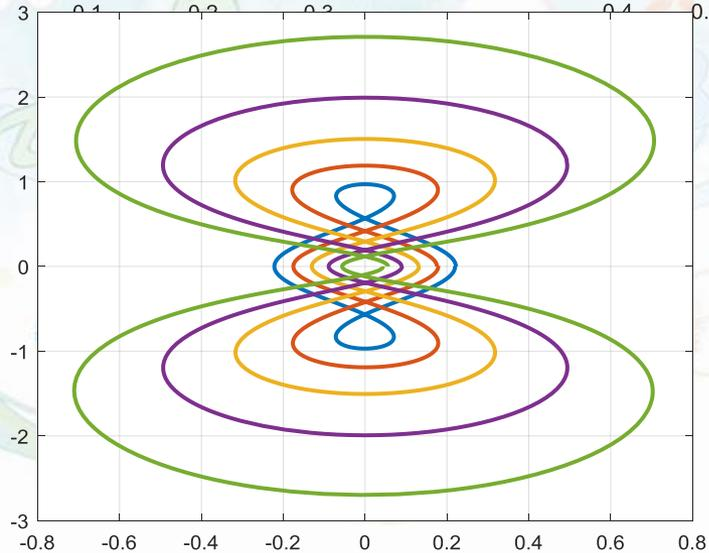
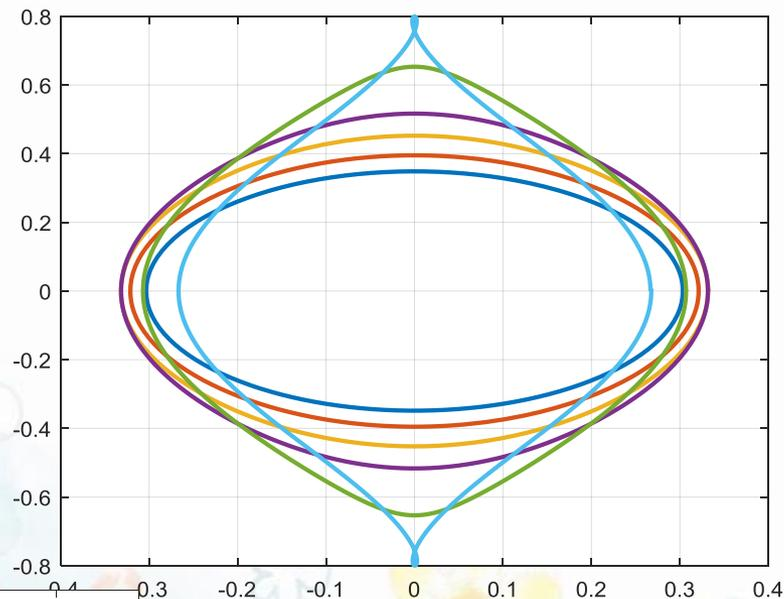


g族

Family g with $\Gamma \geq 4.5$ Stable distant prograde orbits



Family g with $2 \leq \Gamma \leq 4.5$ Unstable prograde orbits



Family g with $\Gamma < 2$: Unstable prograde orbits

DRO轨道任务

- 在木星冰封卫星任务（JIMO）中，木星系统 DRO为航天器在木卫二欧罗巴周围的逃逸和捕获提供了瞬时稳定的转移路径。
- NASA 的小行星重定向任务曾计划将一颗近地小行星捕获到DRO。
- Ocampo 与 Rosborough 提出利用日地系统 DRO部署天基望远镜的应用方案。
- 在欧空局的 DePhine（Deimos and Phobos Interior Explorer）任务中，火星系统 DRO 被用作该项目中火卫一与火卫二基地的备选轨道之一。
- Stramacchia 等提出利用日地 DRO 部署天基望远镜网络探测近地危险小行星。
- 2017 年，NASA 提出将在未来十年内建立一个连接地月空间与深空的空间运输网络。对于深空中长期执行的科学研究任务，稳定及近似稳定的轨道，如DRO、NRHO，是这类任务的潜在应用轨道。

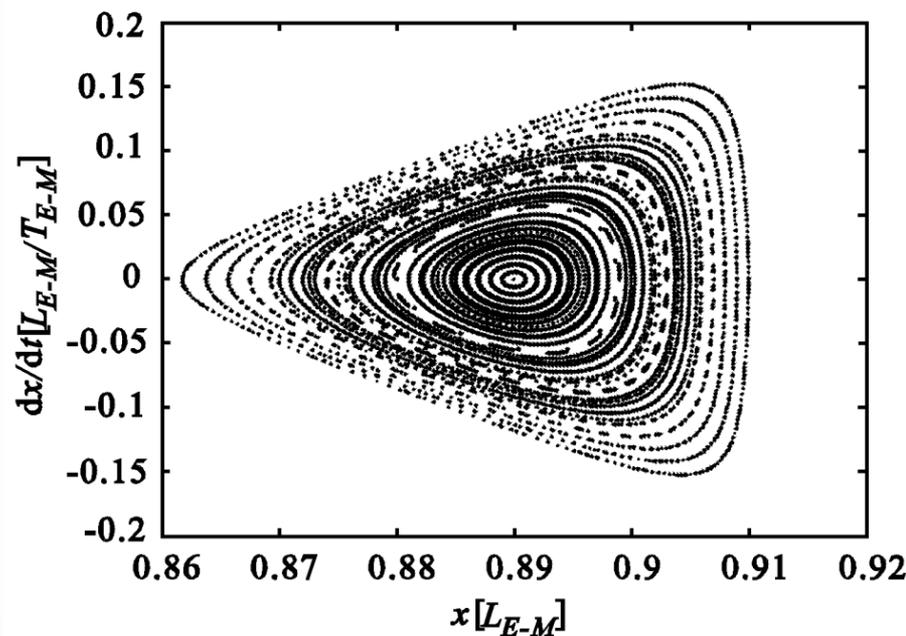
DRO稳定性

Ляпунов稳定性

Poincaré稳定性

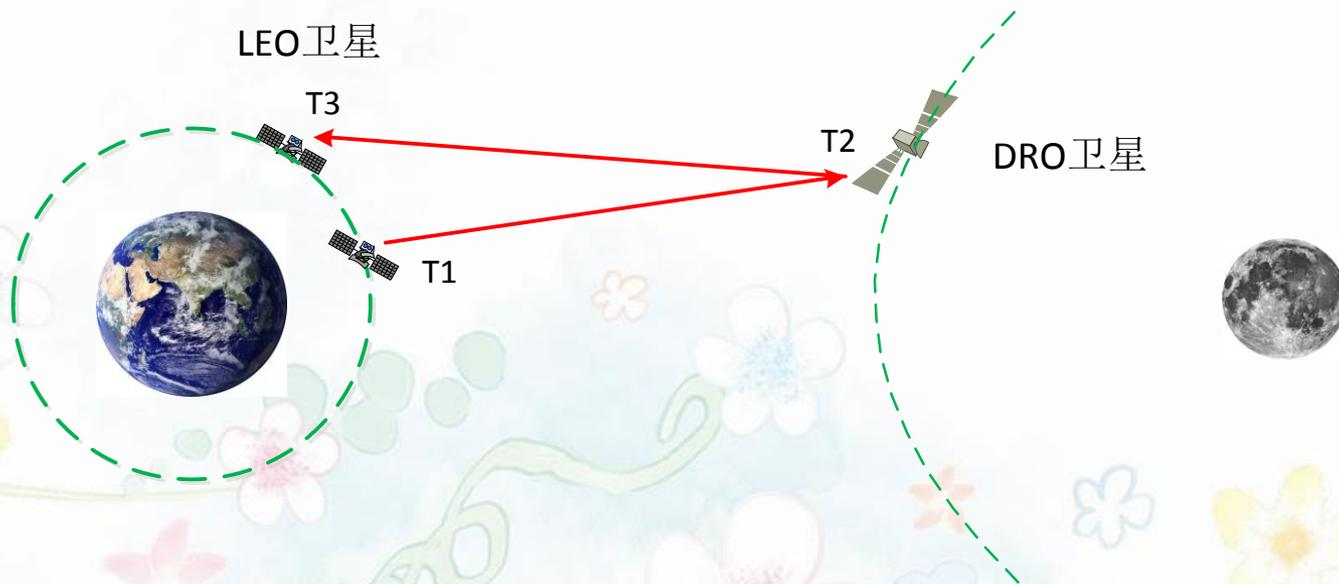
结构稳定性

Bezrouk 研究了稳定性长达 30 年且适合作为地月系统停泊轨道的 DRO 轨道族，距离月心的振幅小于 50,000 km（周期小于 9.3 天）和振幅在 60,000 km~80,000 km（周期 11.6~16 天）的 DRO 轨道的稳定性非常好。即使 DRO 轨道相对于月球公转轨道面存在一定倾角，稳定性也能达到数十年以上。



假设 $f \in C^k$ 有周期轨道 $\gamma(x_0)$
如果它的 Poincaré 映射的所有特征值位于单位圆内，则周期轨道渐近稳定。

LEO双程测量DRO轨道及确定



$$\rho_d = |\mathbf{r}(t - \Delta t_2) - \mathbf{R}(t)| + \Delta \rho_{gr} + \varepsilon_d$$

$$\Delta t_2^{i+1} = \rho_d(\Delta t_2^i)$$

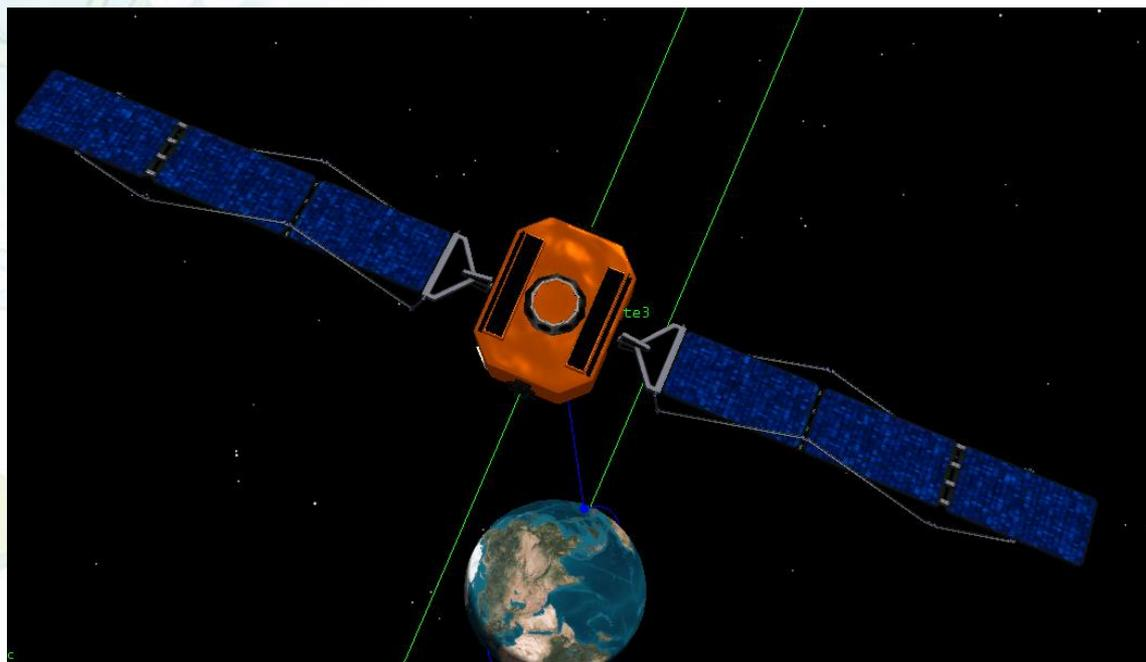
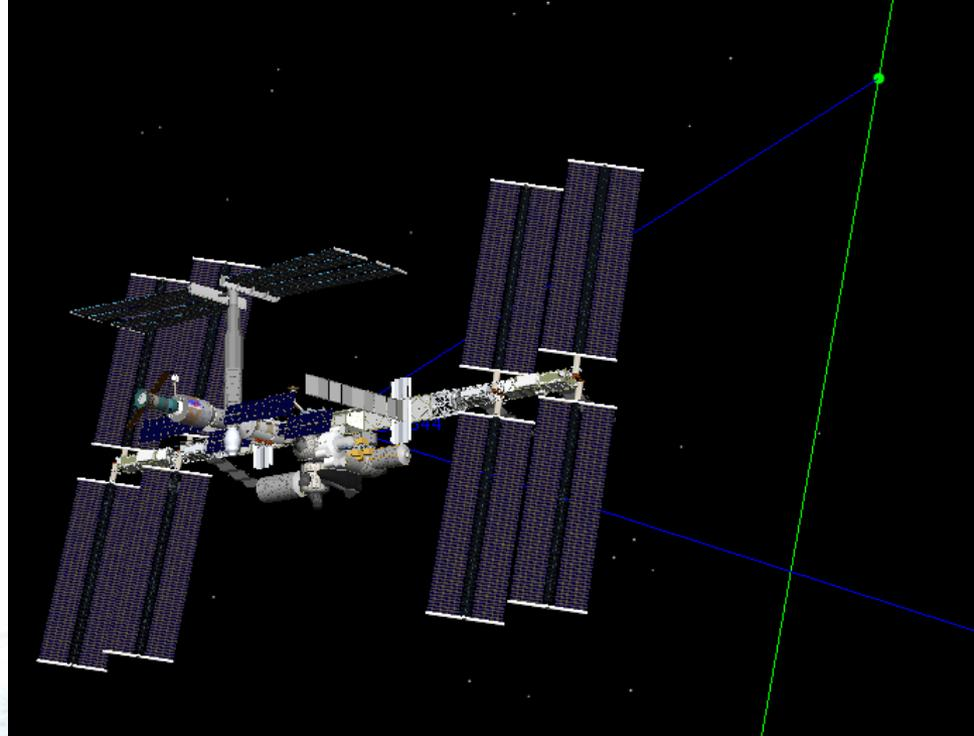
$$\rho_u = |\mathbf{r}(t - \Delta t_2) - \mathbf{R}(t - \Delta t_1 - \Delta t_2)| + \Delta \rho_{gr} + \varepsilon_u = \frac{1}{c} \left[|\mathbf{r}(t - \Delta t_2^i) - \mathbf{R}(t)| + \delta \rho_d(\Delta t_2^i) \right]$$

$$\Delta t_1^{i+1} = \rho_d(\Delta t_2, \Delta t_1^i)$$

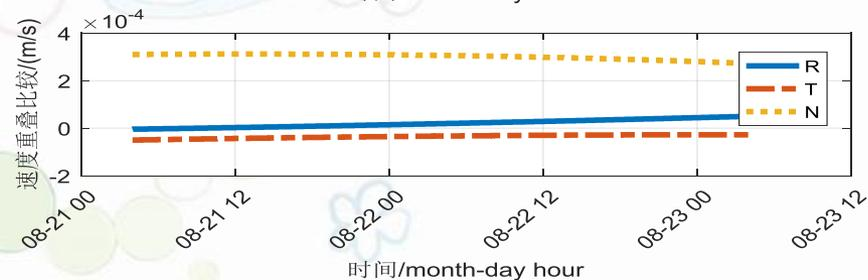
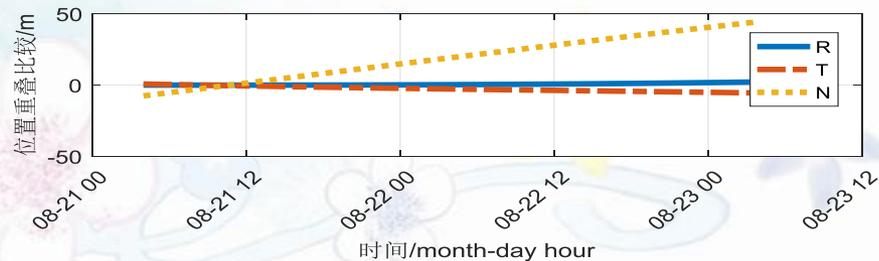
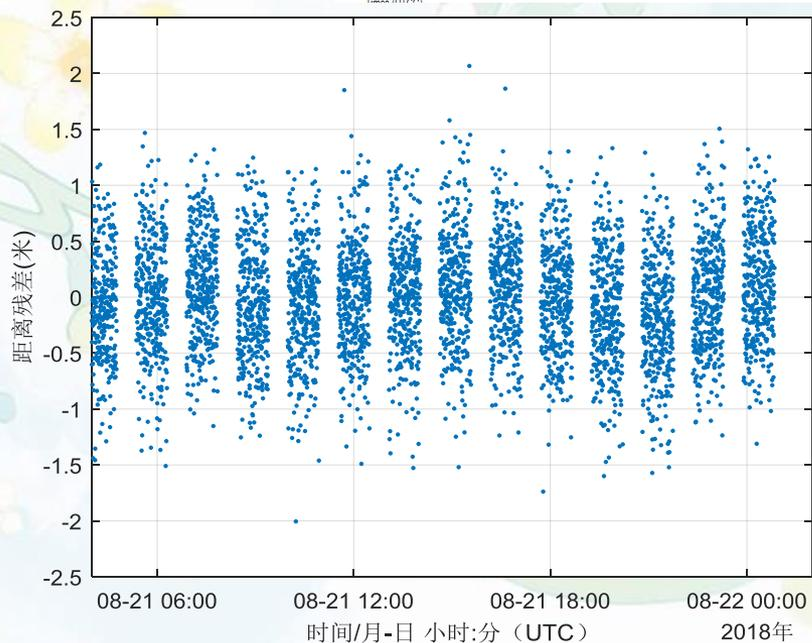
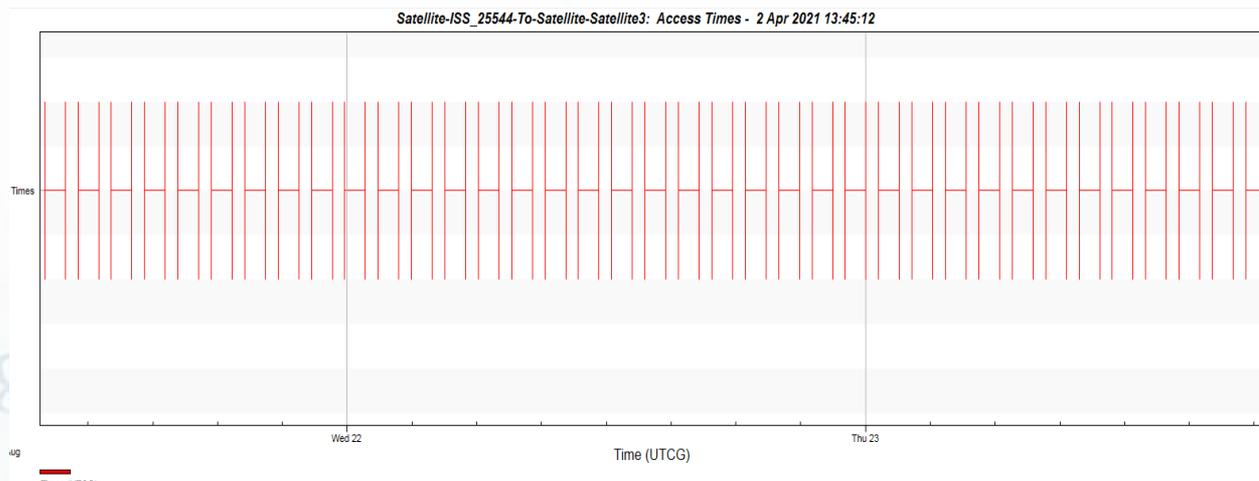
$$= \frac{1}{c} \left[|\mathbf{r}(t - \Delta t_2) - \mathbf{R}(t - \Delta t_1^i - \Delta t_2)| + \delta \rho_u(\Delta t_2, \Delta t_1^i) \right]_{4\theta}$$

仿真条件

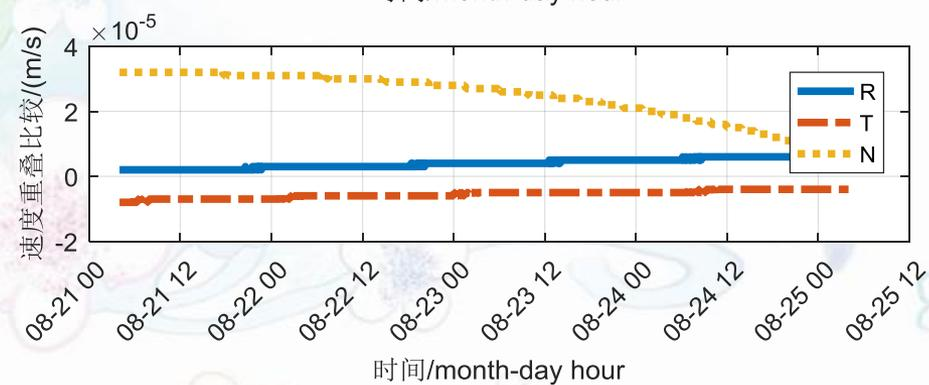
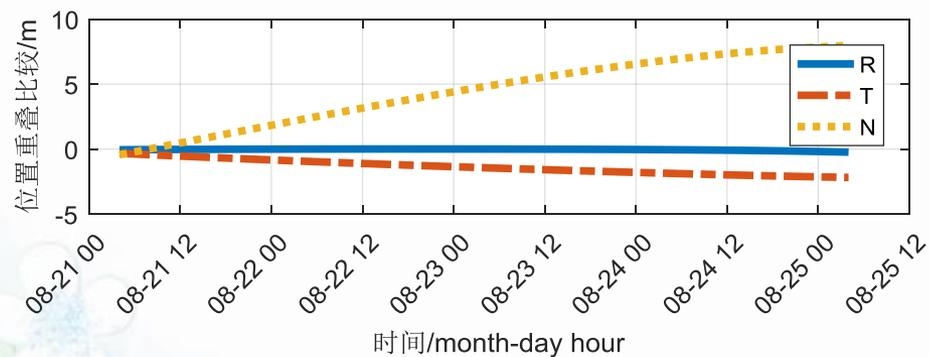
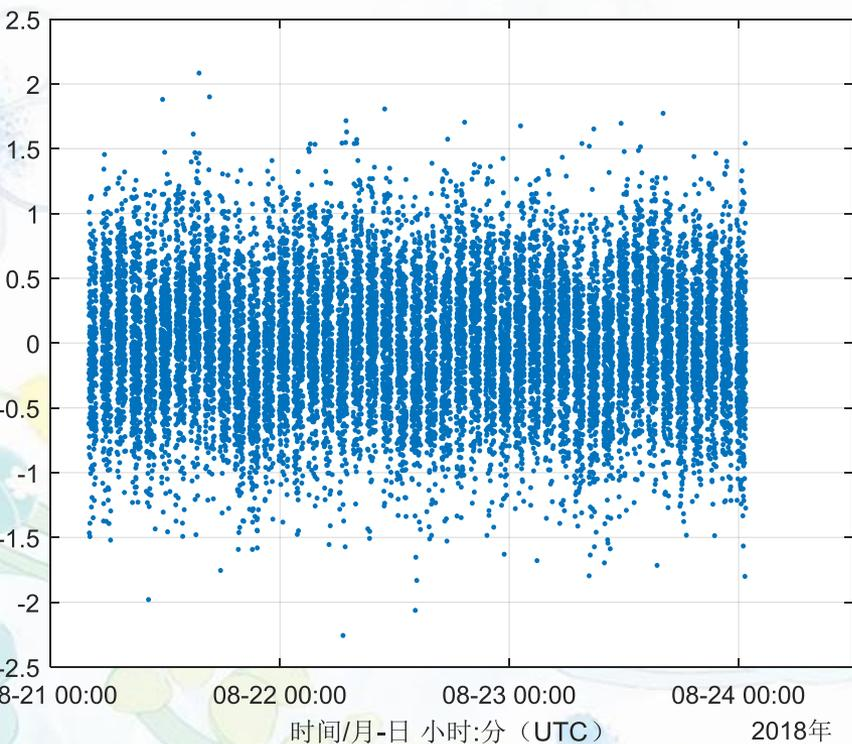
LEO轨道误差	0.5米
测量噪声	0.5米
数据采样率	10秒
引力场	10*10
第三体	DE行星历表
广义相对论效应	后牛顿
光压	估计Cr参数
轨道积分参考系	J2000地心天球参考系
相对论引力时延	Shapiro
积分器	KSG
估值	QR givens-gentleman变换
野值处理	3-sigma



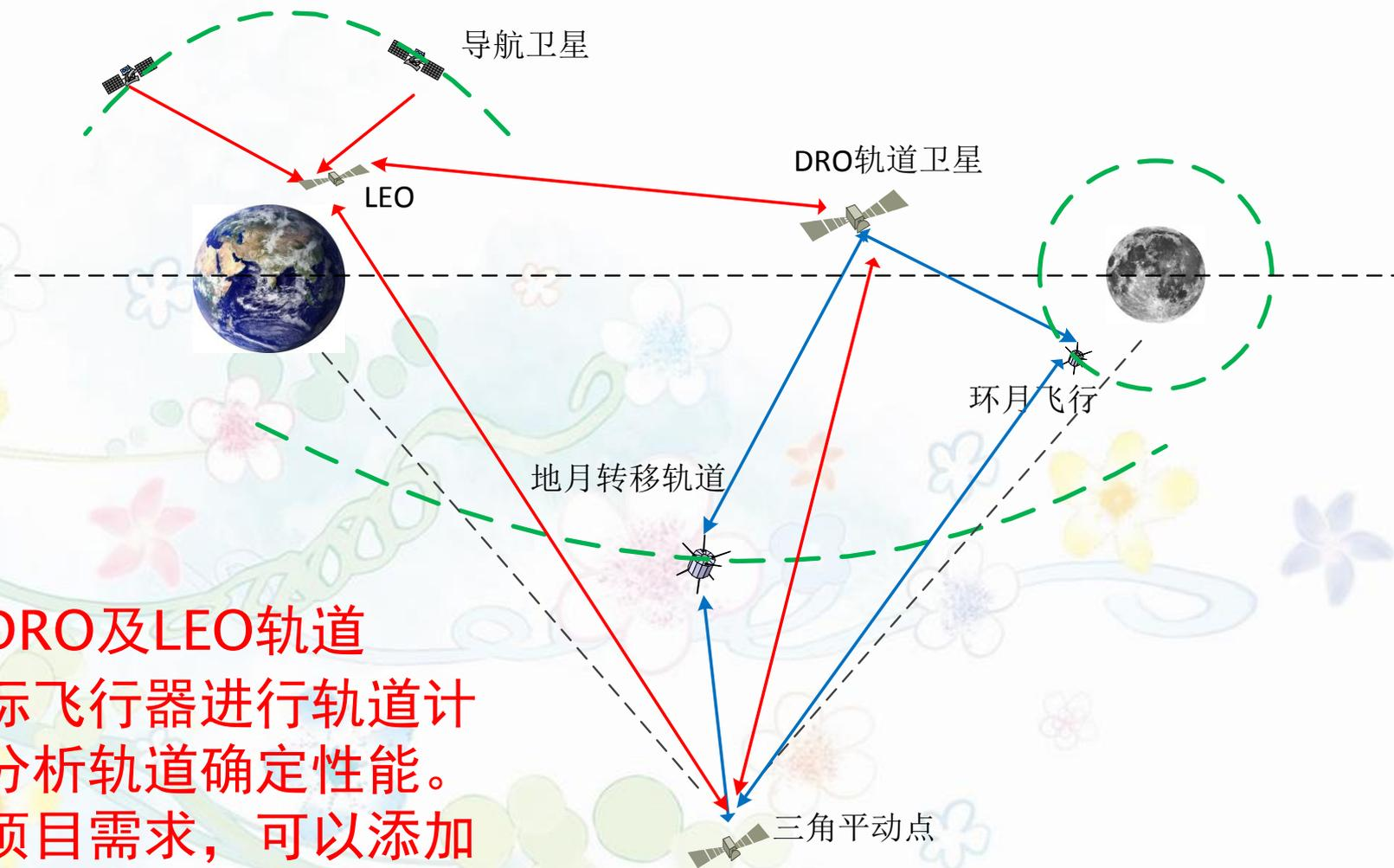
初步定轨结果（1天弧段）



3天弧段



DRO-LEO编队对地月空间飞行导航

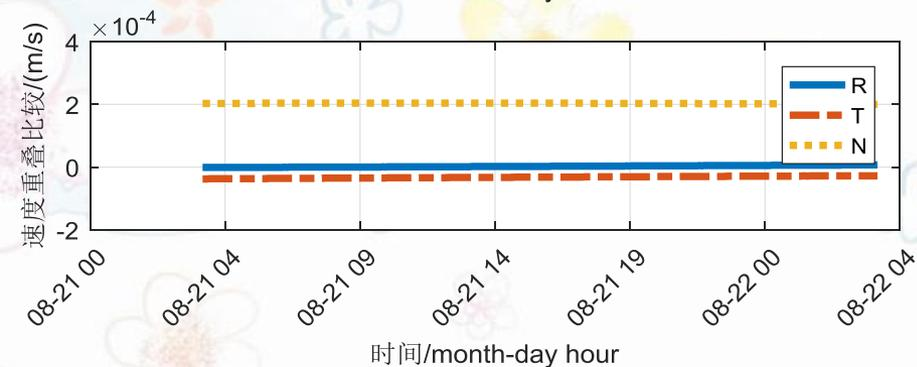
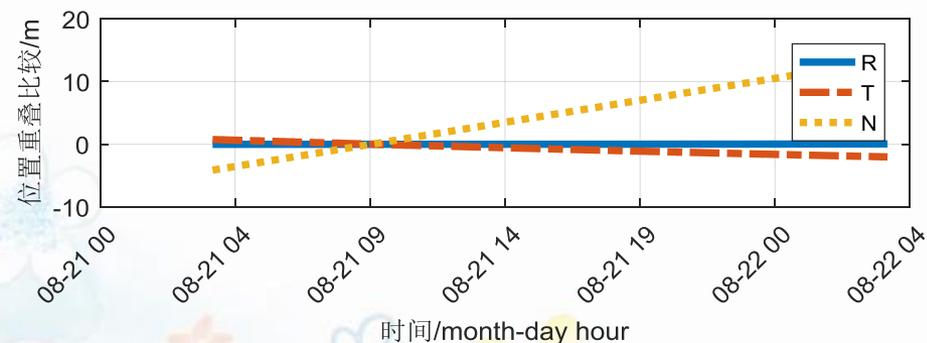
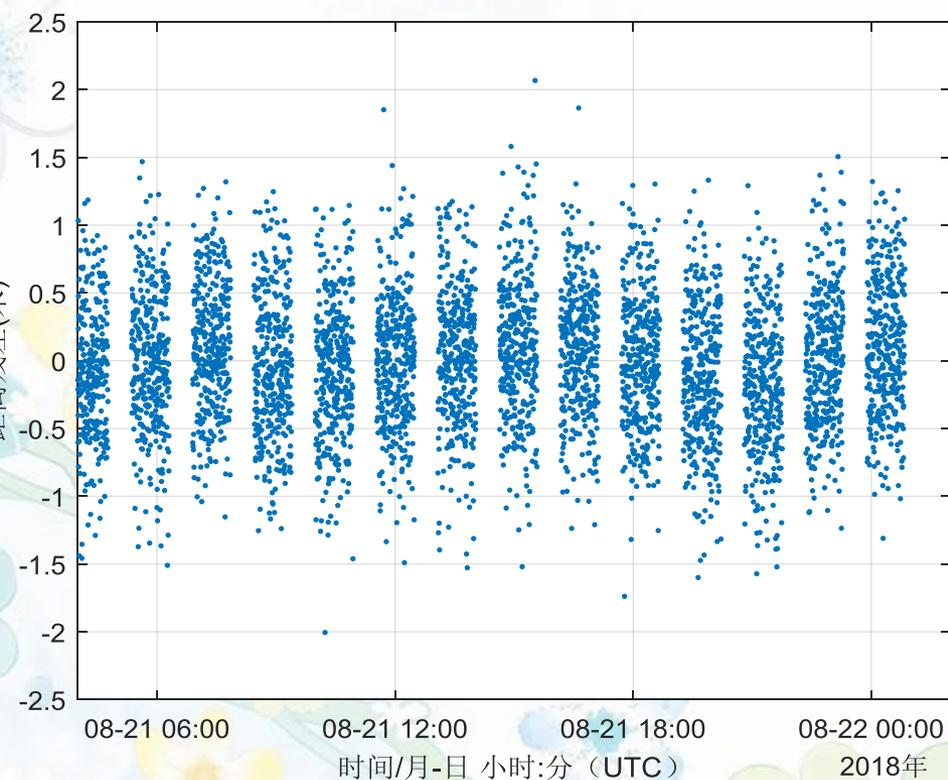


固定DRO及LEO轨道

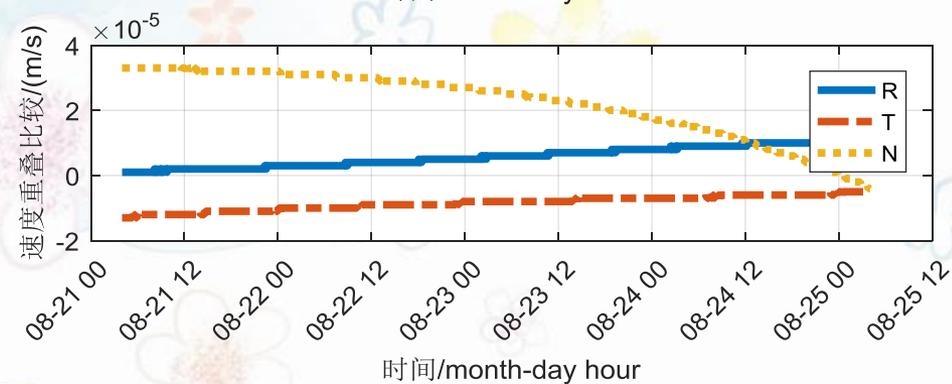
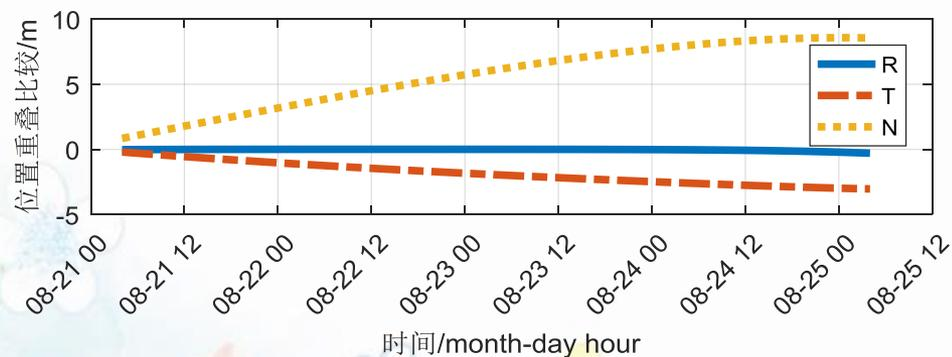
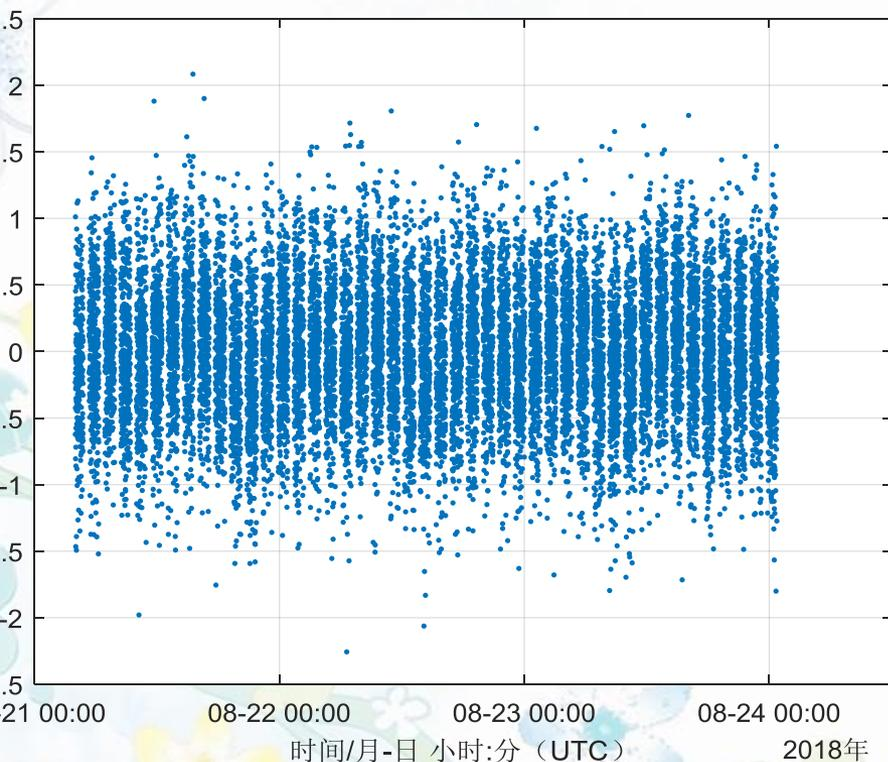
对目标飞行器进行轨道计算。分析轨道确定性能。

根据项目需求，可以添加三角平动点卫星作为中继。

DRO对环月卫星定轨（1天）



DRO对环月卫星定轨（3天）





Q&A!

